Universidade de Lisboa
Faculdade de Ciências
Departamento de Biologia Animal

Expression and function of the transcriptor factor *PROX1* during the development of the gastrointestinal tract

Andreia Sofia da Cruz Margarido

Dissertação
Mestrado em Biologia Evolutiva e Desenvolvimento

2014

Universidade de Lisboa
Faculdade de Ciências
Departamento de Biologia Animal

Expression and function of the transcriptor factor *PROX1* during the development of the gastrointestinal tract

Andreia Sofia da Cruz Margarido

Dissertação
Mestrado em Biologia Evolutiva e Desenvolvimento

Orientadores:

Doutor Pascal de Santa Barbara

Professora Doutora Sólveig Thorsteinsdóttir

2014

ACKNOWLEDGEMENTS

After one year full of experiences and memories there are some people I would like to give a big "Merci" and "Obrigada".

First of all, I would like to thank Pascal for letting me be part of the team and for all the support and enthusiasm throughout the projects. You always gave me some hints that would make me more curious about possible explanations for the results, making me investigate more on the topic and try new experiments. Secondly, I would like to thank Ludo for all the patience. I guess we can say it was a big year for both of us, with two projects, but we ended up reaching something. I've learnt so many techniques and you always tried to teach me how to do it in other experimental conditions. Also, your help and support with this report were essential. Phrases like "It's the final bit" or "You're almost done" were my inside voice in this part of writing the report. To Sandrine, I want to tell you how much your friendship means to me. You always had so much to do and always found time to see my results and discuss what happened wrong or what could I conclude from them. I wasn't directly your student but you were always paying attention. After this year, I feel I really grew a lot as a Person and a Scientist and you know you had a big influence on this growth. In one of our last conversations I noticed that you knew me too well, whether when I was homesick and you hugged me or when I was frustrated with the non-results and you encouraged me to keep going. I have a lot of good memories with you but there's one phrase that you told me that will follow me throughout my professional life: "Science is made of ups but mostly of downs. You have to fully enjoy every good result you have and save it in your memory in order to encourage you when you're facing the downs". With Seb I felt so many times you were like my big brother. All the help with changing houses, contracts, with the red blood cells in microscope and other protocols. I loved all the afternoon conversations with google to help with translations and if I now have some culture on Winter Sports it's thanks to you! What I've told Sandrine is also applicable to you. You treated me like a friend and I miss talking to you. To Stéphane and Jen I want to thank for the good environment we had in the office and lab. I bet Stéphane is now very happy that I'm not next to him. I hope labmeetings still have some cookies at the beginning! I do remember Pascal saying he would cook "Pastéis de Nata" for labmeetings, so I'll be waiting for the picture!

Em relação aos "Obrigada" portugueses, queria começar por agradecer à Professora Sólveig pela amizade, apoio e sinceridade em momentos relacionados com a tese e opções futuras. Chegar à FCUL e entrar no vosso laboratório faz-me sempre sentir em "casa" e lembrar-me dos bons momentos que passei enquanto estive a estagiar no vosso grupo. Ao André um obrigada "por tudo e mais alguma coisa", pelos momentos mais sérios como pelos momentos mais tolos, mas essencialmente por teres estado sempre comigo; à txica Andreia, tenho a agradecer o facto de ter sido promovida de "escrava" a amiga do quotidiano. Quem diria que após me orientares no estágio ainda tinhas de me aturar todos os dias e com desafios de 9 horas de diferença, por isso foi um bom estágio que resultou numa Grande amiga.

À Patrícia e ao Gonçalo um obrigada pelos e-mails de grupo onde também me incluíam, pelas conversas a saber como estava e por me fazerem sentir que desde o estágio nada mudou.

E porque com o fim do Mestrado, termina também um ciclo na FCUL existem muitas outras pessoas a quem gostaria de agradecer por me terem acompanhado ao longo destes 5 anos.

Ao grupinho das meninas (Lili, Té, Lu, Martinni, Kelly, Mi love, Andreia e Joaninha) pelas milhentas gargalhadas e por serem fantásticas. Em especial à Lili queria apenas dizer que "Tu não és para mim senão uma pessoa inteiramente igual a cem mil outras pessoas. E eu não tenho necessidade de ti. E tu não tens necessidade de mim. Mas, se tu me cativas, nós teremos necessidade um do outro. Serás para mim o único no mundo. E eu serei para ti a única no mundo..." (O Principezinho).

Ao maninho Dário e ao senhor Mek só posso dizer que não há tempo nem distância que mudem a nossa amizade, muito menos as gargalhadas que damos juntos.

Por último, mas de extrema importância para mim queria agradecer à minha família. Aos meus pais, pelo eterno amor, enorme apoio e doce carinho. Por me ajudarem a crescer; entenderem que, por vezes, demoro o meu tempo a crescer, mas por sempre terem paciência até que lá chegue. Por acreditarem mais em mim do que muitas vezes eu acredito e por sempre terem lutado pelo melhor para mim. À minha mana, pela amizade, pelas conversas, pelos ralhetes e pelas risadas. Por me saberes sempre "dar a volta" e por estares sempre presente à distância de uma chamada, onde quer que eu esteja. Ao mano Alex pela honestidade, sinceridade e amizade. Aos meus sobrinhos Noahzinho e Liamzinho pela alegria, sorrisos e miminhos que dão à Tia Deia. E aos meus avós e Ciai pelas chamadas e e-mails que tornaram Montpellier numa cidade um pouco mais portuguesa, ajudando a matar as saudades da minha Lisboa.

A todos um sincero OBRIGADA e um forte abraço!

ABSTRACT

The gastrointestinal tract (gut) is a complex organ whose major functions are nutrient and water absorption. Its functioning relies on the coordinated work of many different tissue types such as smooth muscles innervated by the enteric nervous system (ENS), which allow the motility of food intake, while the intestine's epithelium and the lymphatic system (LS) play a key role in nutrient absorption. Thus gut development through embryogenesis requires precise fine-tuning for the establishment and differentiation of all its components. Interestingly, LS and ENS, two components of the gut that will form networks, do not develop intrinsically but rather colonize the immature gut from adjacent tissues. The LS develops from venous endothelial cells inside the cardinal vein that migrate towards VEGFC gradient coming from the mesenchyme. The ENS arises from two distinct populations of neural crest cells (NCC): vagal and sacral. The vagal cells migrate in an antero-posterior direction, giving rise to most of the cells composing the ENS, while the sacral cells migrate inversely, colonizing the post-umbilical part of the intestines.

In this study we found that although these two systems migrate towards the gut from very different locations and at different stages of development, they are both characterized by the expression of *PROX1*, codifying a transcriptor factor with a homeodomain capable of regulating the transcription of other genes. At initial stages (around E5) *PROX1* is expressed in the nerve of Remak (NoR), a structure formed from sacral NCC. Interestingly, colonization of the intestines by this population of cells correlates with *PROX1* downregulation, around E7-8. At later stages (E14) *PROX1* expression is turned on again between the circular and longitudinal muscles, this time labeling the LS. Once specified the LS, *PROX1* expression is always maintained. Between E15 and E18, the LS develops towards the epithelium.

Further studies with *in ovo* and *in vitro* electroporation technique will be done in order to misexpress *PROX1* in the NoR and address its function during ENS development.

Key words: gastrointestinal tract; lymphangiogenesis; *PROX1;* enteric nervous system; sacral neural crest cells.

RESUMO

O sistema gastrointestinal é um órgão vital, complexo e conservado entre os vertebrados. O seu desenvolvimento embrionário inicia-se no estádio HH8 com o aparecimento de uma invaginação na zona anterior do embrião. Em HH13, a segunda invaginação dá-se na zona posterior e estas duas alongam-se até à zona do embrião que se encontra ao nível do saco vitelino. Este tubo primitivo endodérmico é entretanto rodeado por mesoderme e estas duas camadas vão-se desenvolvendo, regionalizando-se em tubo digestivo anterior, médio e posterior. Após todos os processos de diferenciação estarem concluídos, o sistema gastrointestinal divide-se em faringe, esófago e estômago (tubo digestivo anterior), intestino delgado (tubo digestivo médio) e intestino grosso (tubo digestivo posterior). No modelo ave, algumas diferenças existem anatomicamente relativamente ao modelo mamífero: o papo substitui o esófago e as duas partes que constituem o estômago: fundus e antrum correspondem ao proventriculus e moela. O fundus é conhecido como a parte glandular do estômago e o antrum como a parte muscular. Em termos de citodiferenciação, o intestino é composto pela mucosa, submucosa, camadas musculares e serosa. Entre o músculo circular liso e longitudinal situa-se o plexus Auerbach ou mientérico; um segundo plexus existe também na camada submucosa, denominado de Meissner.

Ao longo do sistema gastrointestinal, três grandes vasculaturas desenvolvem-se: sistema cardiovascular, linfático e entérico nervoso. Estas em conjunto com as células do músculo liso permitem que o sistema gastrointestinal cumpra as suas funções de digestão dos alimentos com a respectiva absorpção de nutrientes e água.

O sistema linfático composto por veias, nódulos linfáticos e órgãos linfóides, tem funções ao nível da absorção, mas também na proteção contra agentes invasores e regulação da homeostasia. Embora seja um sistema de alta importância para o trato digestivo, este ainda se encontra por estudar, sendo apenas compreendido ao nível do seu primeiro surgimento na veia cardinal (E9 no modelo ratinho). A sua proximidade com o sistema cardiovascular advém de algumas células localizadas dorso-lateralmente na veia cardinal começarem a expressar *Sox18* que, por sua vez, activa *Prox1.* Uma vez expresso o factor de transcrição *Prox1*, estas células já estão especificadas como endoteliais linfáticas, sendo sempre necessária a sua expressão para que a sua identidade se mantenha. Ao longo do eixo antero-posterior da veia, os conjuntos de células que expressam *Prox1* vão aumentando o número de células a expressarem este gene e iniciam a sua migração em relação a um gradiente químico de VEGFC. O gradiente VEGFC é expresso pela mesoderme lateral e a indução da migração acontece por via de activação e dimerização dos receptores VEGFR3. Embora este receptor seja comum ao sistema circulatório cardiovascular, aquando do momento de migração das células endoteliais linfáticas este receptor não é expresso pelas células endoteliais sanguíneas. Essa migração leva à constituição de sacos linfáticos, que se expandem e fundem com outros sacos linfáticos, formando toda a rede linfática do corpo. A separação entre sistema cardiovascular e linfático acontece por via da expressão do gene *Podoplanina*, codificando uma proteína transmembranar do tipo das mucinas, que promove a

agregação de plaquetas sanguíneas na zona de comunicação entre os dois sistemas. Este mecanismo é conhecido como o mecanismo de desenvolvimento geral do sistema linfático e embora seja responsável pela formação de toda a vasculatura linfática, o modo como ele atinge e se desenvolve nos órgãos está ainda por se determinar.

Um outro sistema também importante para a fisiologia do sistema digestivo é o sistema entérico nervoso. Este sistema é responsável pelo movimento das células musculares lisas, facilitando os movimentos gastrointestinais e fluxo sanguíneo. O seu desenvolvimento dá-se a partir de células da crista neural de duas origens diferentes: vagal e sacral. Estas células encontram-se respectivamente no tubo neural entre os sómitos 1 e 7, e a partir do sómito 28º. Entre o limite do tubo neural e da ectoderme não neural, encontram-se estas células vagais e sacrais que sofrem uma transição epitélio-mesênquima, delaminam do epitélio e migram para o sistema gastrointestinal.

Em galinha, as células sacrais formam uma estrutura externa ao cólon, mas próxima deste, denominada nervo de Remak. A sua extensão é desde o cólon até à parte pós-umbilical e ao contrário das células vagais, elas migram primeiro em direção ao plexus mientérico e somente depois para a submucosa. Esta migração do nervo para o cólon ocorre aproximadamente a E7.5, seguindo-se depois na direcção caudo-rostralmente. O sistema entérico nervoso é maioritariamente derivado das células vagais, mas as sacrais ainda contribuem 17% para a inervação do cólon.

Diferentes vias de sinalização regulam a migração destas células no eixo antero-posterior, sendo as duas mais importantes as vias RET/GFRα1/GDNF e EDNRB/EDN3.

Na via RET/GFRα1/GDNF, o ligando GDNF é expresso no mesênquima do estômago e cecum em diferentes estádios temporais, mas sempre numa posição anterior à frente das células vagais em migração. Este ligando promove a sobrevivência e proliferação dos precursores do sistema entérico nervoso e pensa-se que seja a principal via que regula a migração das células vagais, uma vez que estas expressam o receptor GFRα1. Contudo, na zona do cólon não existe nenhum ponto em que haja expressão significativa de GDNF, o que pode significar que outro mecanismo actue na regulação da migração dos precursores do sistema entérico nervoso nesta zona do sistema digestivo.

A via EDNRB/EDN3 influencia a migração das células precursoras do sistema entérico nervoso. Em ratinho, o ligando *Edn3* é expresso inicialmente nas células mesenquimatosas do tubo digestivo anterior e médio, mas mais tarde restringe-se ao cecum e cólon proximal. O receptor *EdnrB* é, por sua vez, fortemente expresso pelas células da crista neural em migração. Antagonistas deste receptor levam a problemas na migração destas células.

Apesar do sistema linfático e entérico nervoso migrarem de regiões diferentes e em estádios embrionários distintos, neste projecto mostrou-se que são regulados pelo mesmo factor de transcrição *PROX1*. Em estádios precoces (E5), *PROX1* é co-expresso com *SOX10* no nervo de Remak. Por volta de E7.5-E8, a expressão de

PROX1 diminui e desaparece, mantendo-se a expressão de *SOX10* nas células sacrais da crista neural. Esta diminuição é observada tanto ao nível do mRNA como da proteína, sendo que nos estudos de imunohistoquímica o desaparecimento da expressão de PROX1 coincide com a entrada das células sacrais no cólon. Uma vez que *PROX1* é expresso unicamente pelas células sacrais e não vagais, *PROX1* torna-se no primeiro marcador encontrado que é diferencialmente expresso pelas duas populações de células do sistema entérico nervoso. Diferentes técnicas foram realizadas: ablação mecânica e química, *in vivo* e *in vitro* das células sacrais, e todas comprovaram a expressão de *PROX1* por estas células.

Mais tarde (E14), PROX1 surge entre as camadas de músculo liso circular e longitudinal do cólon, desta vez especificando o sistema linfático. Entre E15 e E18, as células endoteliais linfáticas migram das camadas musculares até à submucosa.

Os resultados deste projecto mostram uma regulação temporal de *PROX1* no desenvolvimento dos sistemas entérico nervoso e linfático. Tendo em conta a observação de uma expressão diferencial pelas células da crista neural sacral e vagal, os próximos estudos focar-se-ão na função da expressão de *PROX1* pelas células sacrais. Os estudos de desregulação génica de *PROX1* irão recorrer às ténicas de microinjecção e electroporação e terão como objectivo testar se PROX1 inibe a entrada das células sacrais no cólon.

Palavras-chave: trato gastrointestinal; linfangiogénese; *PROX1;* sistema entérico nervoso; células sacrais da crista neural

TABLE OF CONTENTS

CHAPTER IV: DISCUSSION

Chapter I

INTRODUCTION

I.1. The gastrointestinal tract

The gastrointestinal tract, also called gut, is a complex, specialized and vital organ system responsible for the digestion of food, absorption of nutrients and water, and waste disposal. Its complexity and specialization is achieved during embryonic development through very finely tuned gene regulation processes along the antero-posterior axis, and from contributions of the three germ layers. The endoderm gives rise to the epithelium, the splanchnic mesoderm forms the visceral smooth muscle and ectoderm innervates the gut through neural crest derived cells. Mechanisms of gut development are highly conserved through evolution, and are thus very similar not only in birds and mammals, but among vertebrates in general [1].

I.1.1. Gut morphogenesis, patterning and function

Early development of the digestive tract directly follows gastrulation and starts with a sequence of two endodermal invaginations. The first fold, named anterior intestinal portal (AIP), occurs at an anterior position of the embryo, and is quickly followed by a second fold named caudal intestinal portal (CIP), at the posterior extremity. In the chick model these events take place around HH8 [2] for the AIP, and HH13 for the CIP. These two invaginations elongate and fuse in the middle of the embryo at the level of the yolk stalk around HH24. In the meantime, the splanchnic mesoderm surrounds this primitive endodermal tube, and interactions between these two tissues specify the mesoderm into the digestive mesenchyme [3]. Later on, after the primitive gut has formed, two independent populations of NCC (vagal and sacral) colonize it to form the ENS [4] (Figure 1).

Despite differences in size and shape, organs that compose the gut are similar among vertebrates. A standard gut is initially composed of three parts: foregut, midgut and hindgut, that will later differentiate into pharynx, esophagus and stomach (foregut), small intestine (midgut) and large intestine (hindgut). In most vertebrates, the stomach is divided in two parts: fundus and antrum. The fundus (or glandular stomach) forms the anterior part and it is composed of gastric glands that secret pepsinogen and hydrochloric acid, responsible for hydrolyzing proteins. The antrum (or muscular stomach) forms the posterior part; it has a function of breaking food into smaller pieces. It also possesses specialized glands that secrete protective mucus into the lumen. At the junction of the stomach and the small intestine resides the pyloric sphincter, which controls the food's passage from the stomach to the intestine and prevents reflux from the intestine into the stomach [1].

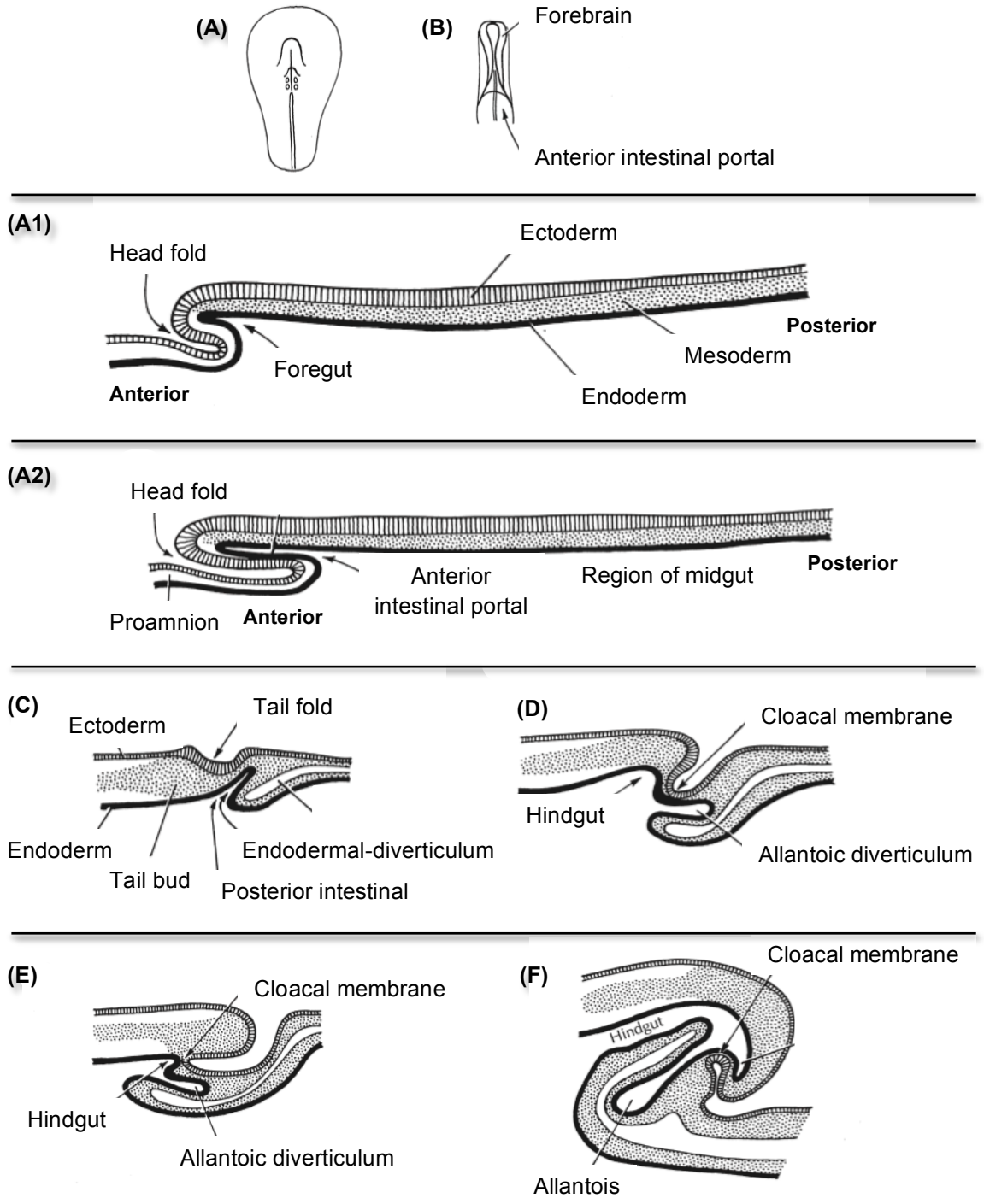

Figure 1 - Gut morphogenesis.
(A) Surface view of an embryo HH7. (A1) Formation of head fold and foregut at HH7 viewed in a sagittal section. (B) Surface view of an embryo HH8. (B1) Sagittal section at HH8, showing a deeper head fold with an increase in foregut length, the anterior intestinal portal. (C-F) Sagittal sections of embryos: HH12-13 (C), HH13-14 (D), HH18 (E), HH20 (F) with the initial formation of posterior intestinal portal that develops into hindgut and later cloaca formation. Images were adapted from [3].

The small intestine is composed of three parts: duodenum, jejunum and ileum, whose distinction is made based on the different cell types composing their epithelial layer [5].

The duodenum is responsible for mixing the food with bile from the gallbladder and pancreatic secretion from pancreas. Bile breaks down fat particles into smaller droplets and pancreatic secretions converts fats into fatty acids and glycerol. Chemical food breakdown is completed in jejunum thanks to a combination of pancreatic enzymes with enzymes produced by the jejunum epithelial wall. The last part of the small intestine (ileum) is responsible for nutrient absorption. Finally, the large intestine is composed of: colon, rectum and anus. Its function is mainly water absorption from the food before the excretion of unused material (feces) out of the body.

Few differences between the standard gut and the gut in the avian model are noticeable: the crop substitutes the esophagus; the two parts that compose the stomach are physically separated into proventriculus (fundus) and gizzard (antrum); cecum is the equivalent of appendix in mammals [1] (Figure 2). The main difference is localized in the posterior part, where the cloaca, that corresponds to a common digestive and urinary chamber that is transient in all other vertebrates, is maintained only in birds [1,6].

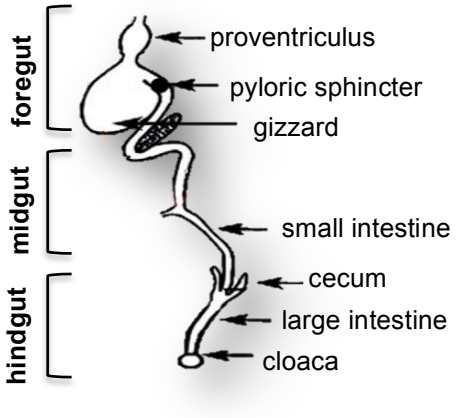

Figure 2 - Gut differentiation along the antero-posterior axis.
Initially the gut is divided into 3 parts: foregut, midgut and hindgut. Later, there is a differentiation of the foregut into proventriculus, pyloric sphincter and gizzard; midgut into small intestine and hindgut into cecum, large intestine (colon) and cloaca. Image adapted from [7].

I.1.2. Gut layer composition and tissue interaction

Despite morphological differences in the organs composing the gut, the radial distribution of tissue layers is similar all along the antero-posterior axis. Four layers can be distinguished: mucosa, submucosa, muscular layer and serosa.

The mucosa is a lamina propria made of connective tissue rich in blood and lymphatic vessels associated with smooth muscle cells. Sometimes the mucosa layer contains glands, lymphoid tissue and a muscular mucosa layer, which is composed of two thin sub-layers of smooth muscle cells separating the mucosa from the submucosa layer. The submucosa is the adjacent layer made of connective tissue, blood and lymphatic vessels, and the Meissner plexus of the ENS. The muscular

layer is made of smooth muscle cells divided in two sub-layers: circular and longitudinal. The circular muscle layer is localized closer to the submucosa; between the two muscles we find the second ENS plexus: the Auerbach's plexus in where blood and lymphatic vessels are also present. Finally, the serous layer (the most external) is a thin layer of connective tissue with blood and lymphatic vessels and a fat tissue that covers a simple squamous epithelium (Figure 3).

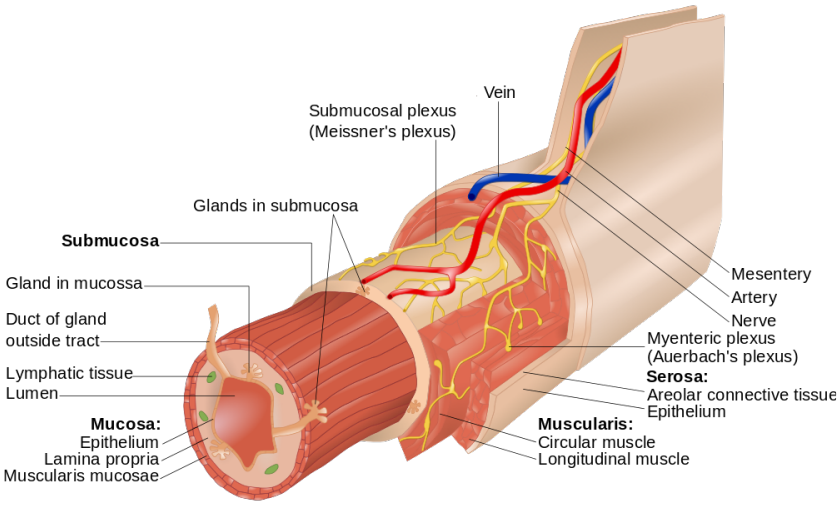

Figure 3 - Gut composition through the radial axis.
From the inner to the outer part of the gut four layers constitute this organ: submucosa, mucosa, muscularis and serosa. Besides the smooth muscle layers it is also visible the LS (green), blood vessels (blue and red) and the ENS (yellow). Image from [8].

Throughout the whole gut, three major networks develop: the blood vascular system, the LS and the ENS. These structures are essential for a proper development of the gut, and they will later play key roles in the functional activity of the gut. The presence of LS within the mucosa and submucosa in association with epithelium protects the organism against bacterial invasion, since it distributes macrophages and lymphoid cells in these regions. Through ENS activity, the muscular mucosa promotes movements of the mucosa, important for contacts between food and mucosa. This facilitates access to food and increases the absorption of nutrients by blood vessels and fat by lymphatic network [9].

I.2. Lymphatic system network

The LS is a vascular network widely spread through the body and intermingled to the blood vasculature. However, despite this overall overlap, these two networks are only connected together at the level of the left sub-clavian vein. The LS is made of vessels, lymph nodes and lymphoid organs [10]. One of the main roles of this network is related to body homeostasis by regulating the volume of interstitial fluid retained in organs. Other essential functions of the LS are: collection of wastes and proteins excess towards the circulatory system, and immune surveillance [11,12]. During lymphangiogenesis, mutation in key regulatory genes lead to major developmental

defects, such as inherited lymphedemas (swelling causing pain due to lymph accumulation in tissues). Finally, a local reactivation of lymphatic development is sometimes observed in and around cancer tumors leading to metastatic propagation of malignant cells to the entire body.

The close proximity to the cardiovascular system arises from its own developmental events. Lymphatic endothelial cells (LEC), the cells that compose the LS are first specified from a subpopulation of blood endothelial cells (BEC) localized dorso-laterally in the paired cardinal veins. LEC specification starts in these cells with the expression of *Sox18* (E9 in the mouse), which in turn activates *Prox1,* the key regulator of lymphangiogenesis [13-15]. At any point in development, a loss of *Prox1* expression causes these cells to lose their lymphatic identity returning to a blood endothelial cell fate and causing aberrant junctions of lymphatic vessels with blood vessels [16]. As soon as they are specified, LEC form clusters of *Prox1* cells along the antero-posterior axis of the vein. These clusters augment their number of *Prox1* cells and migrate through VEGFR3/VEGFC signaling, forming small sacs that will later expand and fuse together, to constitute lymph sacs [17]. The protein Podoplanin (PDPN) a mucin-type transmembrane glycoprotein is responsible for platelet aggregation, cutting connections between the cardinal vein and lymph sacs which results in the separation between blood and lymphatic vessels [18] (Figure 4). It is still not clear whether the whole lymphatic vasculature is derived from these lymph sacs or if other processes are involved.

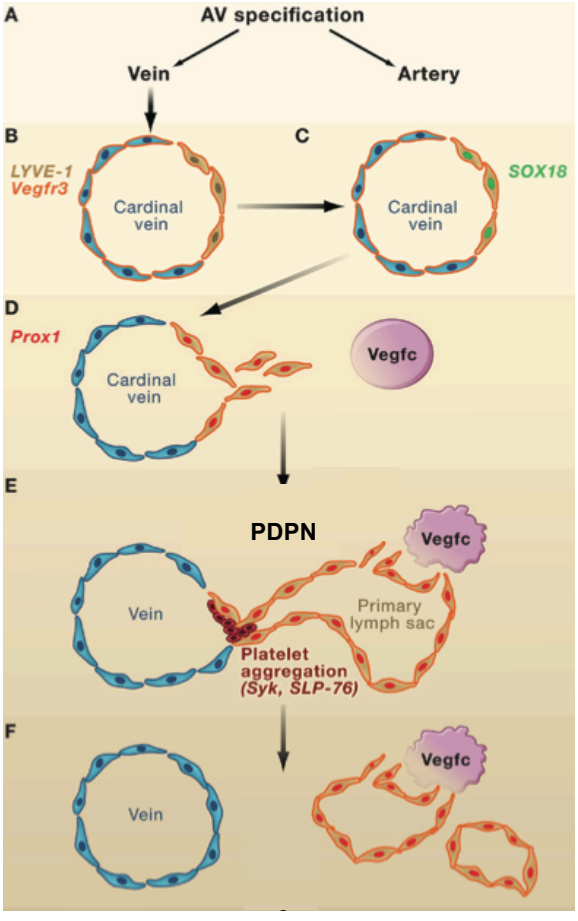

Figure 4 - Events of lymphatic system development.
(A-C) After artero-venous specification, some cells present in the dorso-lateral part of the cardinal vein start expressing *LYVE-1* and *SOX18*. At this developmental time both blood vessels and LEC express *VegfR3*. While *Prox1* is expressed, *VegfR3* is downregulated in BEC and maintained strongly expressed in LEC, which permits their migration towards the increasing VegfC gradient (D). As migration proceeds lymph sacs form and progressively isolate from the cardinal vein due to platelet aggregation caused by PDPN (E). All the lymphatic vasculature is established from lymph sacs proliferation and fusion to each other (F). Image adapted from [13].

VEGFR3/VEGFC signaling can both activate BEC and LEC but when lymphatic vessels start sprouting from the cardinal vein, VEGFR3 is downregulated in BEC. VEGFC binds to VEGFR3 provoking a dimerization with another VEGFR3, which activates two signaling pathways: PI3K-Akt and ERK. As seen in Figure 5 a downregulation of ERK by Akt activity can serve as a critical control in LEC sprouting and also contribute to LEC differentiation and maintenance of lymphatic activity [19].

These mechanisms describe how specification, determination and expansion of the LS occur. However, how this system migrates into specific organs, such as the gut still needs to be determined.

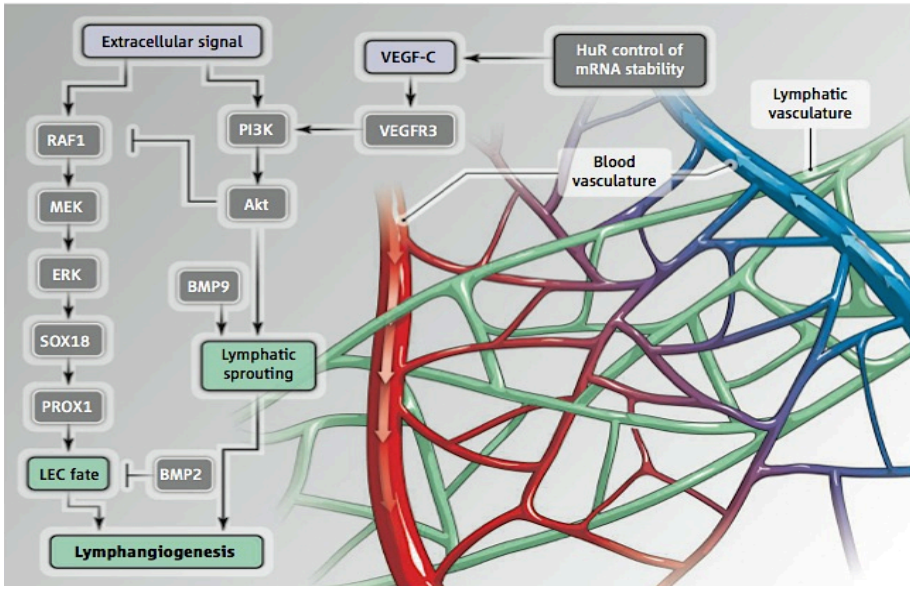

Figure 5 - Signaling pathways involved in lymphangiogenesis.
VEGFC binding to VEGFR3 induces its dimerization, which provokes the activation of two signaling pathways: PI3K-Akt and ERK. Akt downregulates ERK functioning as a control to maintain LEC sprouting and its differentiation. BMP2 signaling pathway also affects lymphangiogenesis, inhibiting LEC fate. Image from [19].

I.3. Enteric nervous system network

The ENS, also called “second brain", is formed by neurons and glia that innervate the entire gut. This system coordinates gut motility and blood flow, and modulates endocrine and immune functions, all commanded partly by the central nervous system [20].

The ENS is organized into two plexi: Meissner and Auerbach which display different localizations. Meissner's plexus is present within the submucosa layer while Auerbach's is situated between the circular and longitudinal muscle layers.

The ENS arises from NCC, cells present at the boundary of the neural plate and non-neural ectoderm that undergo an epithelium-mesenchymal transition (EMT) and delaminate from the epithelium, migrating through specific pathways [21]. NCC are

multipotent stem cells that will give rise to different cell types such as melanocytes, bone and cartilage of the face, or enteric neurons and glia depending on their localization along the neural tube.

Two types of NCC form the ENS of the gut, the vagal NCC and the sacral NCC.

Vagal NCC migrate ventrally from the neural tube located at the level of somites 1-7 at embryonic day 3 (E3). They first accumulate in caudal branchial arches before entering by the foregut mesenchyme. Inside the gut their migration goes rostro-caudally reaching the posterior end around E8-E8.5 in chicken embryos [4,22]. Interestingly, their migration behavior within gut mesenchyme changes along the antero-posterior axis. In the pre-umbilical gut, vagal NCC are evenly distributed within the mesenchyme, while in the post-umbilical gut they migrate in the outermost layer of the mesenchyme. Finally, when they reach the hindgut, they colonize first the inner submucosa layer. The exact reasons for this behavior are not clear but it seems that this is linked to mesenchyme differentiation into muscles [23].

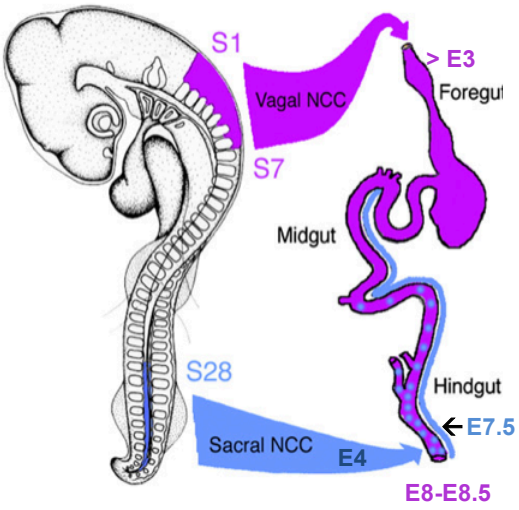

Figure 6 - Enteric nervous system ontogeny.
Vagal NCC arise from neural tube close to somites 1-7 and sacral NCC from somite 28th caudalwards. Vagal NCC colonize the entire gut and sacral NCC only migrate until the post-umbilical gut. Image adapted from [24].

Sacral NCC are present on the neural tube from somite 28th and caudalwards; at E4 they migrate ventrally to form a structure specific to birds called the Nerve of Remak (NoR). This nerve develops exterior to the gut but in close proximity to it. It extends from the posterior end of the hindgut to the anterior limit of the post-umbilical gut. At E7.5 these cells migrate out of the NoR entering the hindgut. They first form a part of the myenteric plexus before spreading to the submucosa plexus. In contrast to vagal cells, sacral NCC migrate in a caudo-rostral manner. These cells only colonize the post-umbilical gut, contributing in 17% of hindgut's ENS. Thus vagal NCC give rise to the greatest part of ENS [22] (Figure 6).

These mechanisms of EMT, migration, and differentiation undergone by NCC require very precise gene regulation, and cell-cell interactions [25]. A failure in any of these steps will severely impact ENS formation and will lead to one of the many pathologies associated to ENS development defects. The most known congenital obstructive disorder is the Hirschsprung's (HSCR) disease, characterized by an incomplete formation of ENS (agangliogenesis) in the distal intestine. Unfortunately, mechanisms leading to this pathology are poorly understood, and there is a need to better understand its development, and the contribution of these two populations of NCC to the innervation of the distal gut. To date, no marker allowing to distinguish vagal from sacral NCC, has been found.

I.3.1. Signaling pathways involved in antero-posterior migration of neural crest cells

The HSCR disease is the most common and most studied congenital ENS pathology. Patient analyzes have identified two relevant pathways: RET/GFRα1/GDNF and EDNRB/EDN3 with major importance in signaling through the RET receptor, as heterozygous mutation in *RET* are found in 50% of familial and sporadic cases. On the other hand, *GDNF* and *GFRα1*, have either rarely been found or never been described in HSCR cases. Regarding the second implicated pathway. Mutations in the second pathway, *EDNRB* and *EDN3,* are found in 5% of HSCR cases [26].

Starting with RET/GFRα1/GDNF signaling, RET is a receptor tyrosine kinase with two isoforms: RET9 and RET51 that bind to Glial-cell-line-derived neurotrophic factor (GDNF) through GPI-linked co-receptor GFRα1. While mice expressing only the *RET9* isoform are phenotypically normal, those only expressing *RET51* lack enteric ganglia, similar to HSCR disease [27,28]. *In vitro* studies have shown that RET ligand, GDNF is a chemoattractant that promotes survival and proliferation of ENS precursors cells that later differentiate into enteric ganglia [29-32]. In mice, *Gdnf* expression occurs within gut mesenchyme in two regions (called hot spots): stomach and cecum mesenchyme [33,34]. The appearance of these two hot spots is temporary separated and always occurs spatially ahead of the vagal NCC wavefront. This together with the fact that GDNF is a chemoattractant and that vagal NCC express *Gfrα1*, indicate that these hot spots attract vagal NCC, inducing a colonization movement throughout the gut. However this mechanism is not applicable to the hindgut, since no hot spot has been found caudal to the cecum [8] (Figure 7).

Interestingly, an *in vitro* study using HEK-293T cells misexpressing *RET* [36] showed that in the absence of RET ligand GDNF, cells suffer apoptosis. They found that this receptor is a dependent receptor: in the presence of its ligand (GDNF), positive signals are sent to induce ENS proliferation; while the absence of GDNF binding, provides negative signals that initiate a pro-apoptotic program. This finding brought new insights into the understanding of HSCR disease, since this disease could be caused by specific mutations in *RET* that lead to problems in sensing GDNF gradient or by the absence of a chemoattractant gradient of GDNF without mutations in *RET*.

The second identified pathway: EDNRB/EDN3 pathway regulates NCC migration inside the gut. Endothelin-3 (EDN3) is a ligand in a family of secreted peptides and binds to 7-transmembrane G-protein coupled receptor, Endothelin receptor-B (EDNRB).

In mice, *EdnrB* is expressed in gut mesenchyme as well as in migrating NCC where its expression is stronger. As for *Edn3,* it is widely expressed in foregut and midgut mesenchymal cells but is later restricted to cecum and proximal colon [37,38]. Several studies have shown the importance of this pathway in NCC migration inside the gut mesenchyme. In mice, a loss of function mutation for one of these genes cause agangliogenesis in the distal gut [8], and antagonists of EDNRB where shown to affect NCC migration, also causing distal agangliogenesis [39] (Figure 7).

Other roles for this pathway where shown in various studies such as: decreased number of neural crest stem cells in guts of *Edn3*$^{-/-}$ mice compared to wild-type [37]; or inhibition of neurogenic and gliogenic lineage commitment in EDN3-treated NCC with a mimicked effect seen in *Sox10* overexpression [40]. Altogether, these results indicate a role in controlling neural crest stem cells and an interplay between EdnrB and Sox10 signaling pathways [41,42].

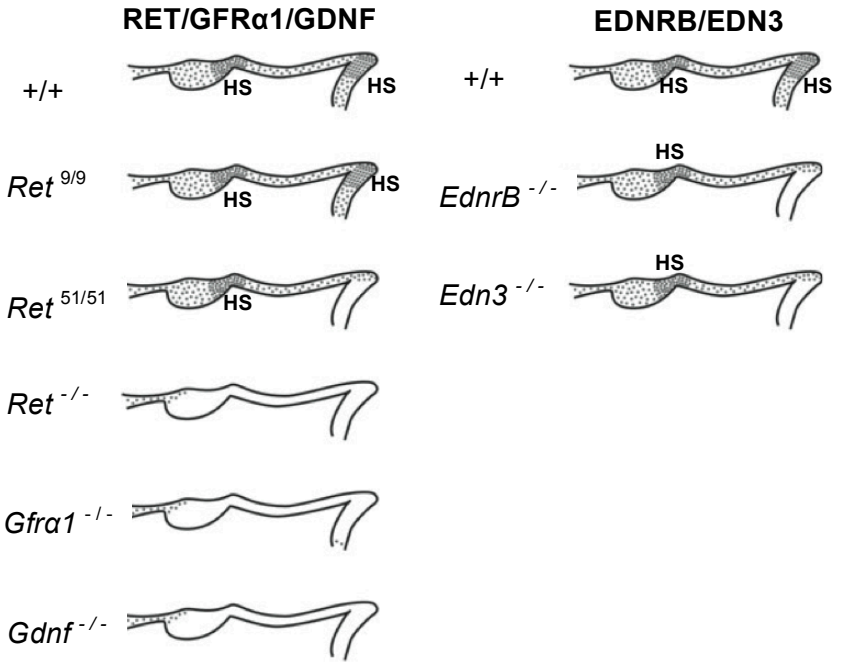

Figure 7 - **Phenotypes of mice with mutations in RET/GFRα1/GDNF and EDNRB/EDN3 signaling pathways.**
Grey dots represent NCC colonization throughout the gut. HS= hot spot.
Figure adapted from [35].

I.4. Objectives

Most developmental studies on LS development have addressed the initial formation and migration of LS precursors from the cardinal vein. In contrast, LS arrival to organs, in particular the gut, still needs to be elucidated. In order to fill this gap, our first goal was to describe the temporal and spatial arrival of the LS into the colon.

In the second part of our study, we focused on *PROX1* expression in sacral NCC, and investigated its function in the potential regulation of their entrance into the hindgut.

Chapter II

MATERIALS AND METHODS

II.1. Embryo collection

Fertilized White Leghorn chicken eggs (*Gallus gallus*) were obtained from Haas Farm in France and incubated in a humidified atmosphere at 38ºC. Embryos were collected at the desire embryonic day of gestation (E) and their stage confirmed with Hamburger and Hamilton staging [2].

II.2 *In situ* hybridization (ISH) probe production

II.2.1. Total RNA isolation and cDNA production

Total RNA was isolated from an E6 whole embryo using the RNeasy Midi Kit (Qiagen). The RNA extract was diluted in RNase free water (Sigma-Aldrich); concentration and purity were measured with a spectrophotometer. RNA was stored at -80ºC until needed for cDNA production. The cDNA production protocol is described in Annex A1 (RT-PCR). cDNA was stored at -20ºC.

Primer design for the RNA probes *LYVE1, PODOPLANIN, PROX1* and *SOX10* is detailed in Annex A2. *CLAUDIN5* probe was kindly given by Dr. Aimee Ryan.

The PCR reaction protocol and PCR product ligation into plasmids, bacteria transformation and plasmid amplification and extraction are all described in Annex A3-A5.

II.2.2. Plasmid linearization and purification

For plasmid linearization, 10 µg of plasmid was digested with 10 U of a restriction enzyme during 2 hours at 37ºC (Annex B, Table B4). The efficiency of digestion was visualized on a 2% agarose gel. Purification of the digested DNA was performed using the kit Nucleospin Gel and PCR clean-up (Macherey-Nagel).

II.2.3. Probe transcription and purification

1 µg of the linearized plasmid (in a maximum volume of 5 µL) was incubated at 37ºC during 2 hours with 2 µL of transcription buffer 10X (Roche), 1.2 µL of DIG nucleotide mix (Roche), 1.2 µL of DTT (Invitrogen), 1.2 µL of RNASE out (Invitrogen), 2 µL of RNA polymerase (Annex B, Table B4) and RNase free water up to a final volume of 20 µL. After the digestion reaction, 2 µL of DNASE (Roche) was added to the

reaction for 10 minutes at 37ºC, and stopped on ice. Probe size was monitored on a 2% agarose gel.

Probe purification was performed using MicroSpin™ G-50 Columns kit (GE Healthcare), eluted in a final volume of 30 µL. Its concentration was measured with a spectrophotometer and stored at -20ºC.

II.3. *In situ* hybridization

Guts dissected from E6 to E16 chick embryos were fixed with 4% paraformaldehyde (Electron Microscopy Sciences) in PBS (4% PFA), fixation time depending on sample's size/developmental stage (Annex B, Table B5). A quick wash was done with PBS 1X (BioWhittaker) followed by a second wash equal in time to the fixation time. From this step on, all the timings were equal to those used for fixation. Then, dehydration was performed with increasing concentrations of methanol diluted in 1X PBS (PBS). Guts were stored in 100% methanol at -20ºC until use.

Day 1

Guts were rehydrated with decreasing concentrations of methanol-PBS for 10 minutes each (or 20 minutes in case of guts from older embryos). Two washes with PBS were done and samples were left for exactly 1 hour in a solution of 6% H_2O_2 (Sigma-Aldrich)-PBS to diminish their endogenous alkaline phosphatase activity. Subsequently, they were washed 3 times in PBT (0,1% Tween-20 in PBS) and incubated with Proteinase K (VMR) in a dilution of 1:1000 (incubation time was adjusted according to embryo stage - Annex B, Table B6). A 10 minutes wash was done with PBT-glycine in a concentration of 2 mg/mL, followed by 2 washes of PBT and a 20 minutes post-fixation in 0,2% glutaraldehyde-4% PFA. Samples were then washed 2 times in PBT and placed 1 hour at 70ºC in warmed **hybridization solution**. Finally, samples incubation with probes was done at 65ºC overnight at a concentration of 70 ng/mL.

Day 2

Embryos were washed 3 times, 30 minutes each, with a pre-warmed **solution 1** at 70ºC, followed by 3 washes, 30 minutes each, in **solution 2** at 65ºC. Next, 3 washes of 5 minutes were done with Tris-Buffered Saline (TBS) 0,1% Tween-Levamisole **(TBST-Levamisole)** (1:100) followed by a blocking of 2,5 hours in 10% fetal bovine serum (Sigma-Aldrich) in TBST-Levamisole done at room temperature with agitation.

During this time, antibody blocking was also prepared by adding a small amount of embryo powder (Annex A6) to 1mL of TBST-Levamisole and incubated for 30 minutes at 70ºC. A quick vortexing was performed and the solution was cooled on ice. The anti-Digoxygenin antibody coupled with alkaline phosphatase (Roche) was added to this solution and centrifuged for 10 minutes at 1000 rpm and 4ºC. The supernatant was collected and mixed in a TBST-Levamisole-1% fetal bovine serum solution, added to each vial, and incubated overnight at 4ºC rocking. The final concentration of the antibody was 1:2500.

Day 3
3 washes of 5 minutes were done with TBST-Levamisole, followed by 5 washes of TBST-Levamisole each during 1 hour with agitation. The final wash was left with agitation overnight at 4ºC.

Day 4
2 washes, 10 minutes each, were performed with Trizma hydrochloride solution 0,1M pH=8 (Sigma-Aldrich)-LT (1:100) diluted in **DEPC-treated water**. Probes were detected using BM purple (Roche) supplemented with LT (1:100). Depending on the embryo stage of the gut and the probe, 1 to 2 days of developing were necessary to be concluded. The enzymatic reaction was stopped in PBS, and tissues were stored at 4ºC in 4% PFA.

II.4. Embedding and cryosectioning

Samples for cryosectioning were fixed for 1 hour in 4% PFA, washed with PBS and left overnight in **solution T1**. On the next day, **solution T2** was added to samples and incubated overnight. Finally, **solution T3** was pre-warmed at 37ºC before being added to samples. Vials with this solution were left during 1 hour in water bath, being agitated once in a while. Once samples were incorporated in blocks with solution T3, they were frozen using isopentane cooled (-30/35°C) with dry ice and stored at -80ºC. Sectioning was performed using a MICROM HM 560 cryostat. Sections were 8 µm thick, were collected on StarFrost microscope slides (Knittel Glass) and slides were left to dry overnight at room temperature for better section adherence.

II.5. Immunohistochemistry

Slides were washed twice in PBS, 10 minutes each, and permeabilized for 10 minutes with 0,1% Triton-X100 (Prolabo VWR) in PBS. The blocking was done using 5% donkey serum (Sigma-Aldrich) in PBS during 30 minutes. Primary antibodies were used at the following dilutions: anti-human PROX1 rabbit polyclonal (Reliatech GmbH) 1:200, TUJ1 mouse monoclonal (COVANCE) 1:400, α-SMA mouse monoclonal (Abcam) 1:300. These dilutions were done in 1% donkey serum in PBS and incubation was done overnight at 4ºC.

Two washes of PBS, 15 minutes each, were performed on the slides to remove the primary antibodies. Secondary antibodies Alexa 488-conjugated donkey anti-mouse IgG and Alexa 555-conjugated donkey anti-rabbit IgG (Invitrogen, Molecular Probes) were diluted 1:400 in a solution of 1% donkey serum in PBS with Hoescht 1:1000 (Invitrogen) and put on slides during 2 hours. 2 washes of 10 minutes each were done and slides were mounted with mounting medium for fluorescent samples (Dako).

II.6. Image acquisition and treatment

Whole-mount guts processed for ISH were photographed with a stereomicroscope connected to a Nikon-AZ100 digital camera and immunohistochemistry images were acquired with a Zeiss AX10 Imager.M1 microscope connected to an AxioCam MRm. ImageJ and Adobe Photoshop CS6 softwares were used to analyze and treat all images.

II.7. Organ Culture

II.7.1. Gut collection

For this experiment 4 groups of samples were created: *in ovo* E6.5, BAC-treated organ culture, organ culture control and *in ovo* E8.5.

All eggs were incubated at the same time and taken out from the incubator when they reached E6.5. Dissection was performed in fresh PBS and whole gut isolation was used for ISH protocol. From this dissection 3 groups were formed: *in ovo* E6.5 group, BAC treated organ culture group and organ culture control group. *In ovo* E6.5 group was immediately fixed in 4% PFA and dehydrated and eggs that were not opened were placed back in the incubator to constitute the last group (*in ovo* E8.5). After 48 hours of incubation organ cultures were washed with PBS and fixed/dehydrated. Meanwhile, the *in ovo* E8.5 group was dissected and samples fixed/dehydrated.

II.7.2. Organ culture proceedings

The 2 culture conditions: BAC and control were washed in DMEM (Dulbecco's Modified Eagle Medium; Gibco) supplemented with 1% Penicillin/Streptavidin (BioWhittaker, Lonza), 2% Hepes 1M (BioWhittaker, Lonza) and 2% L-Glutamine 200mM (Sigma-Aldrich) (Medium 1). The BAC group was incubated for 10 minutes in a Benzalkonium chloride solution (Sigma-Aldrich) and then washed 3 times with medium 1. The Benzalkonium chloride solution was at a concentration of 0.04%. Both groups were incubated at 37ºC for 48 hours in a differentiation medium. This medium was prepared from medium 1 supplemented with 0,02% BSA (Euromedex) and insulin at a concentration of 1 µL/mL.

II.8. Quantitative RT-PCR

RNA isolation and reverse transcription were done as described in section II.2.1 and Annex A1**.** 1 µg of RNA was used as a template for the reverse transcription reaction.

For each well the following mix was prepared 2.5 µL of cDNA, 1.5 µL LightCycler480 SYBR Green I Master water (Roche), 1 µL of mixed primers 0.5 µM (Annex B, Table B7) and 5 µL of 2x LightCycler480 SYBR Green I Master (Roche). RT-PCR amplification was run with a LightCycler technology (Roche Diagnostics; 95°C for 10

seconds, 60°C for 10 seconds, 72°C for 15 seconds) and mRNA quantification was determined by LightCycler analysis software (version 3.1).

II.9. Western-Blot

Proteins from E15 pancreas samples were extracted by adding 200 µL of **Laemmli 4X buffer** for 5 minutes at 100ºC. A final disruption of the tissue was done with a pipette.

Samples were loaded into the **stacking gel** through which they ran at 80V before being separated in the **running gel** for about 80 minutes at 120V in **1X running buffer**. Proteins were then transferred into a nitrocellulose blotting membrane (GE Healthcare) using **1X transfer buffer** for 1 hour at 100V. The membrane was washed with TBS with 0,1% Tween20 (TBST) and blocked with 5% Skim Milk (BD Difco) in TBST for 30 minutes. Three washes were done with TBST before adding the primary antibody diluted in 5% Skim Milk in TBST overnight. The anti-human PROX1 rabbit polyclonal (Reliatech GmbH) was used at a concentration of 1:1000.

Four washes of TBST 5 minutes each were done to rinse the antibody. The anti-rabbit antibody coupled to the horseradish peroxidase (Bethyl laboratories) was diluted 1:5000 in 5% Skim Milk in TBST and incubated with the membrane for half an hour. Three quick washes with TBST were done and the enhanced chemiluminescent substrate from the Western Blotting Luminol Reagent kit (Santa Cruz Biotechnology) was put in contact with the membrane for 1 minute. The developing was done in darkness by exposing the membrane to a high performance chemiluminescence film (GE Healthcare) inside a cassette with BioMax MS Intensifying Screen (Kodak BioMax) for 20 seconds.

II.10. Electroporation

II.10.1. Plasmid injection

PROX1 and ΔDBD-*PROX1* (*PROX1* without its DNA-binding domain) plasmids were kindly given by Dr. Panagiotis Politis [44] while, U2-*DTA* (*SOX10* enhancer expressing diphtheria toxin) plasmid was given by Dr. Christophe Marcelle [45]. Plasmid pCIG4 was also used to express *GFP* (Annex D3).

For each experiment, there were always 2 groups: control and injected. Control group was only injected with pCIG4, while injected group was injected either by *PROX1* or ΔDBD- *PROX1* or U2-*DTA*, together with pCIG4.

PROX1, ΔDBD-*PROX1*, U2-*DTA* and pCIG4 were used at a concentration of 2 µg/µL. pCIG4 when used together with another plasmid was at 1 µg/µL.

II.10.2. *In ovo*

Embryos were first incubated for about 2.5 days until stage HH16. Injections were done in the neural tube, with a microinjector at the level of somite number 25 and caudalwards. After microinjection, gold plated electrodes from Cell Porator Electroporation System ECM 830 (BTX) were placed on either side of the neural tube and the electroporation was performed at 25V (3 pulses of 5ms). Electroporation was done bilaterally. Eggs with electroporated embryos were put back in the incubator and dissected out at E6.5. Colons were dissected and only the ones showing fluorescence were kept for later analysis. Tissue analysis was done either by quantitative RT-PCR or immunofluorescence.

II.10.3. *In vitro*

Embryos were dissected at E6 and only colons were kept. Electroporation was performed in the NoR and as previously described. Colons were cultured in organ culture in the same differentiation medium as used in section II.7.2. After 2 to 4 days, colons were taken out from culture, washed with PBS and processed for immunofluorescence.

II.11. Sacral neural crest cells ablation

A window was opened after 2.5 days of incubation at stage HH16. From somite 25 down to the most posterior part, neural tube was ablated (without touching the notochord) using the microinjector needle. Once ablated eggs were placed back in the incubator and allowed to reach stage E6.5. Control colons were let incubated until E6.5 without neural tube ablation. Colons were then dissected and processed for immunohistochemistry assays.

Chapter III

RESULTS

III.1. Gut lymphatic system development is a late embryonic event

To determine when the LS arises in the gut, whole-mount ISH was performed from early (E5) to late (E16) stages of gut development, for genes specific of the different endothelial subtypes. *LYVE1*, *PROX1* and *PODOPLANIN* were used to characterize the LS, while *CLAUDIN5* was used as a general endothelial cell marker, meaning that this gene is expressed in both blood and LS (Figures 8 and 9).

This comparison among vasculatures revealed a difference in their timing of establishment. While the blood vasculature has already developed throughout the whole gut at E12 (Figure 8A-C), at that stage no markers of the LS are present within the gut mesenchyme (Figures 9B-D). In Figure 9B, two lymphatic vessels are observed in the mesentery. Both vasculatures are easily distinguishable in bright field (Figure 9A).

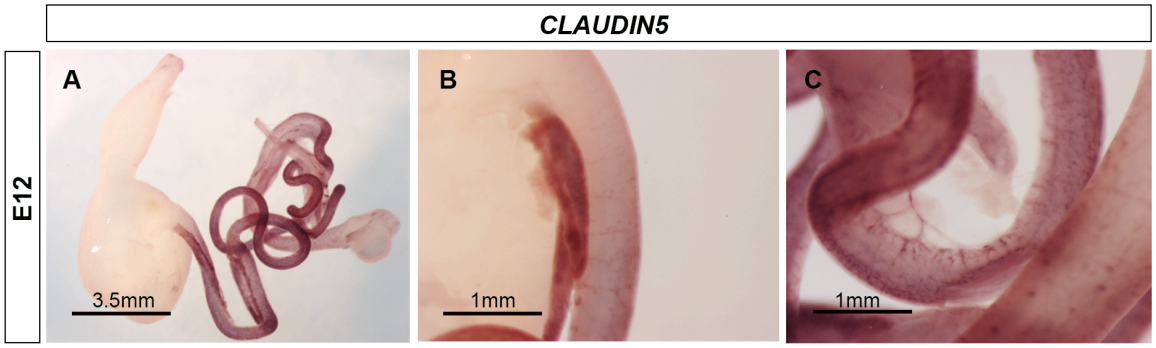

Figure 8 - *In situ* hybridization analysis of vascular network development in the intestine and associated mesentery.
At E12 a well developed blood vasculature is already present in mesentery and intestine (A-C).

At E13, two large vessels located along the gut express lymphatic markers (Figures 9F-H). These two vessels most likely are lymphatic collecting vessels (Figure 9E).

Starting from E14, cells expressing lymphatic vessel genes decrease in number. At E14, gene expression still occurs in large vessels (Figures 9J-L), whilst at E15 no expression is visible (Figures 9N-P). At E16, formation of smaller vessels can be seen in Figures 9Q-S.

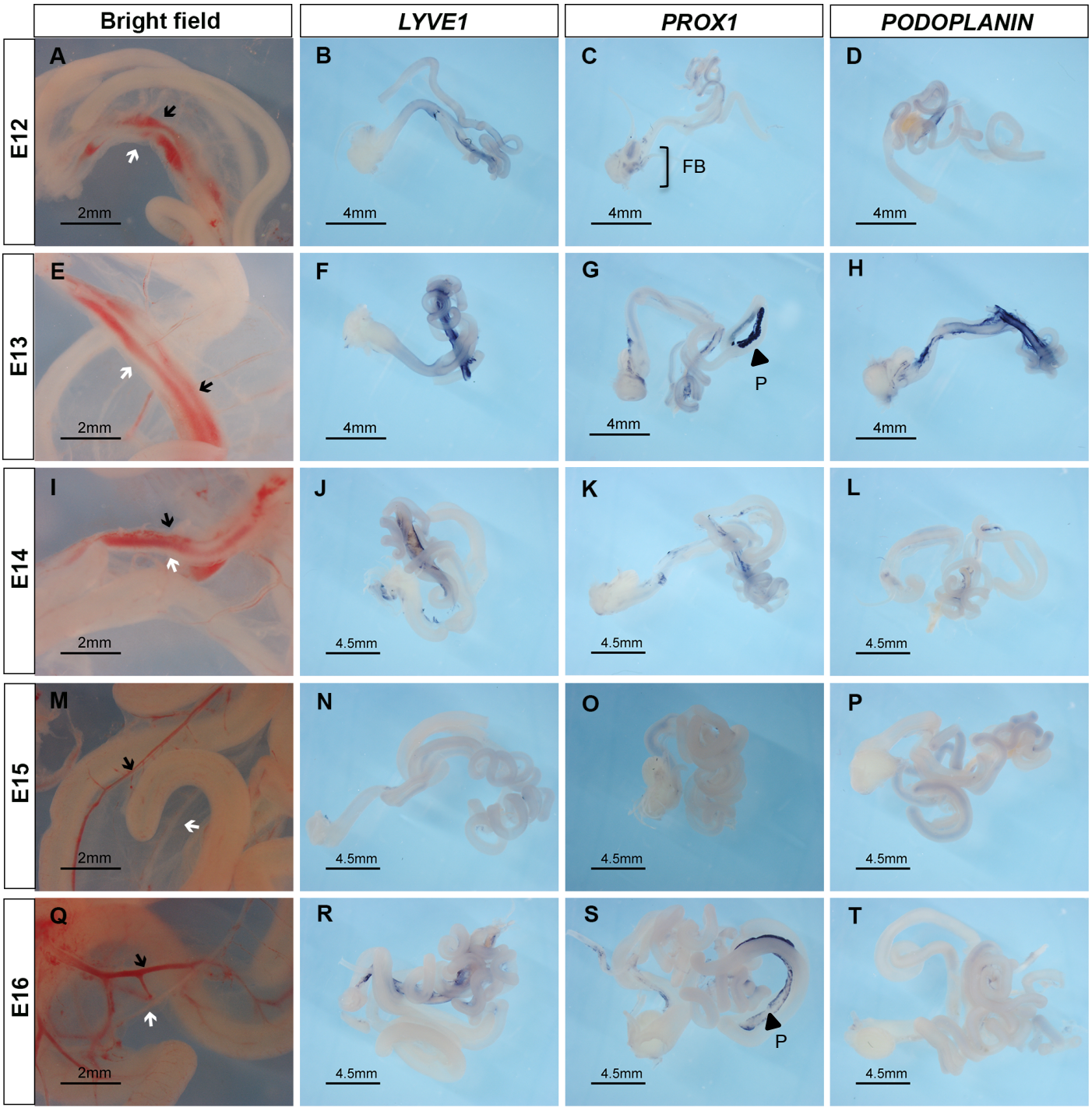

Figure 9 – *In situ* hybridization analysis of lymphatic network development in the intestine and associated mesentery.
Bright field visualization of the mesenteric vasculature (A,E,I,M,Q) and ISH in whole-mount embryo guts for *LYVE1* (B,F,J,N,R), *PROX1* (C,G,K,O,S) and *PODOPLANIN* (D,H,L,P,T) from E12 to E16. Starting at E12, both blood (Figures A,E,I,M,Q, black arrows) and lymphatic (Figures A,E,I,M,Q, white arrows) vasculatures have developed and are in close proximity. *LYVE1, PROX1* and *PODOPLANIN* are strongly expressed in mesenteric lymphatic vessels at E13, but their expression decreases after that. The Fabricius bursa (FB, Figure C, brackets) and pancreas (P, Figures G and S, black arrowheads) are positive controls for *PROX1* expression.

Although, *LYVE1* (Figures 9B and F) and *CLAUDIN5* (Figure 8) are both expressed in the intestine mesenchyme, only *CLAUDIN5* (Figure 8C) depicts the formation of a typical vascular network. *LYVE1* expression in the mesenchyme is only found at these two stages, and given the fact that later during development the probe stains lymphatic vessels, this mesenchymal expression is likely due to other functions not related to the lymphatic vasculature.

In addition, *PROX1* expression appears in a chicken-specific lymphoid organ, the Fabricius bursa (FB, Figure 9C, brackets), and in the pancreas (P, Figure 9G and S, arrowheads). *PROX1* has been shown to be involved in the development of the exocrine pancreas [46].

III.2. Colon lymphatic network forms after the establishment of the mesenteric vasculature.

As the technique of whole-mount ISH shows its limits when studying tissues so late during development, we decided to look for the presence of protein by immunofluorescence. No lymphatic-specific antibodies developed for the chicken model are currently commercially available, however we decided to test three different antibodies directed against human proteins: PROX1, LYVE1, and PODOPLANIN. First, we characterized PROX1 antibody by performing a Western-Blot and an immunohistochemistry assay into an organ known to express *PROX1*: the exocrine pancreas at E15 (Figure 10). The methodology used to extract nuclear proteins does not allow protein quantification in the sample, thus we have loaded growing volumes of protein extract in the different wells.

In all samples we observed one band with an estimated size between 70 and 100 kDa according to the protein ladder; which corresponds to the expected chicken PROX1 protein size of 83 kDa (Figure 10A). In addition, in an immunofluorescence assay (Figures 10B'-B") the PROX1 antibody stains the exocrine pancreas in a pattern similar to what has been reported in the literature validating the antibody specificity [46]. Characterization assays conducted with LYVE1 and PODOPLANIN antibodies showed no cross-reaction on chicken samples (data not shown).

In our immunofluorescence assays, we used the PROX1 antibody in combination with the αSMA antibody to visualize the smooth muscle layer surrounding blood vessels. Cross-section through these major vessels present in the mesentery associated with the gut (Figure 11) show an extensive and intricate lymphatic network in close vicinity with blood vessels (Figure 11A'"). As previously observed (Figure 9), gut lymphatic vasculature develops at late stages. Techniques of ISH in the chick gut have shown their limits after E12 due to organ thickness and subsequent difficulty in probe accessibility to the target RNA. Furthermore, due to the very few number of cells present in thin capillary structures of the lymphatic system, ISH in sections resulted in a very poor staining (data not shown). However, we know that a lymphatic system is required for gut functions such as absorption and immunity matters [13].

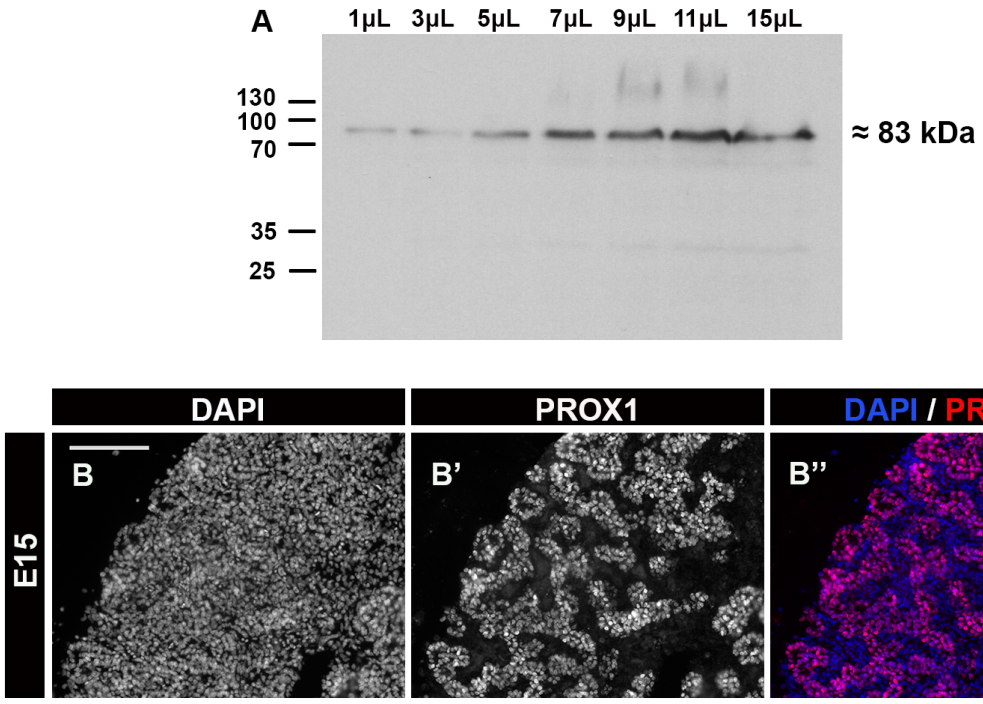

Figure 10 - Characterization of PROX1 antibody in the chicken model by Western-Blot and immunohistochemistry.
PROX1 antibody specificity was tested using a protein extract from an E15 pancreas in Western-Blot and E15 pancreas sections for immunohistochemistry. Western-Blot analysis shows one specific band at the predicted PROX1 protein size of 83 kDa (Figure A). On the immunohistochemistry assay, the exocrine pancreas expresses PROX1 (Figures B',B"), validating our antibody. http://www.reliatech.de/fileadmin/ds/pa/102-PA32AG.pdf.
Scale bar: 100µm.

To overcome these technical limitation of the ISH protocols, we decided to take advantage of the PROX1 antibody that we characterized and to look for PROX1 protein expression patterns by immunohistochemistry assays. Using PROX1 in combination with αSMA or TUJ1, we were able to visualize the lymphatic network between the muscle layers in order to investigate its potential relationships with the blood vascular system and ENS.

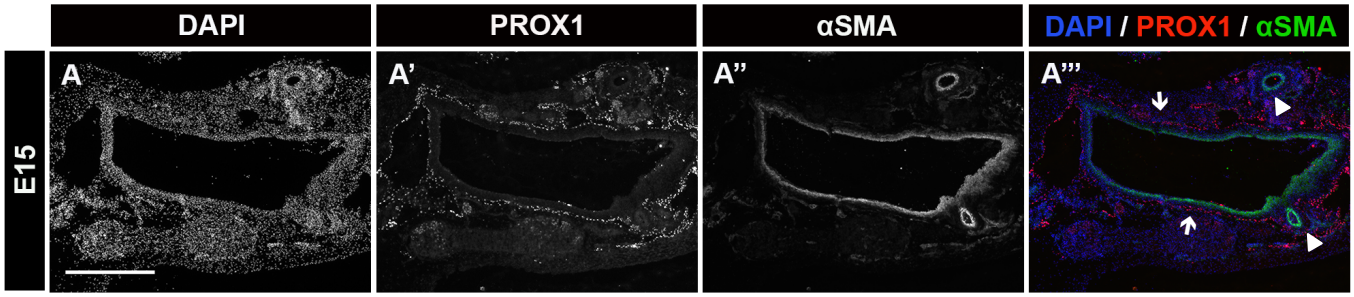

Figure 11 – Blood and lymphatic vessels are closely associated in the mesentery.
Immunohistochemistry assays on sections were done with antibodies against PROX1 (Figure A' and red channel in Figure A''') and αSMA (Figure A'' and green channel in Figure A''') on E15 exterior vasculature along the colon. Lymphatic endothelial cells form an extensive network (Figure A''', arrows) in proximity to blood vessels (Figure A''', arrowheads).
Scale bar: 500µm.

We performed immunohistochemistry assays at the same developmental stages used in the ISH studies (E12 to E15). As seen in Figures 12B''-H'' and in accordance with the literature [47], the αSMA antibody stains three smooth muscle layers, termed longitudinal muscle layer (LM), circular muscle layer (CM) and muscularis mucosa layer (MM) (Figure 12B''). We can also observe the smooth muscle cell layer surrounding blood vessels (Figures 12C'' and D'', arrowheads). Red blood cells are unspecifically stained in both green and red channels, showing an orange/yellow color (Figures 12F'''-H'''). Regarding PROX1 staining, at E13 no lymphatic network is present in the gut though some positive cells are observed outside the colon (Figure 12B''', arrow). At E14, some LEC have started to enter the colon from the outer vasculature into the space between the longitudinal and circular muscle layers, staying next to the blood vasculature (Compare Figure 12C'' arrowhead to C''' arrow and D'' arrowhead to D''' arrow).

At E15, the lymphatic network pattern is similar to E14 (Compare Figure 12D''' with E'''). PROX1 is expressed in some epithelial cells (Figure 12F''', arrows) but these are not involved in lymphatic vessel formation and labeled some neuroendocrine epithelial cells. At E18, the lymphatic network has already been developed throughout the entire colon; it has entered and passed the circular muscle layer (Figure 12G''', arrow) and spread down to the muscularis mucosa muscle layer (Figure 12H''', arrow).

Therefore, in E15-E18 interval of time, the lymphatic network expands from the vessels present among the longitudinal and circular muscle layers down to the muscularis mucosa muscle layer.

In a second part we investigated lymphatic system development with relation to the ENS establishment (Figure 13).

Inside the gut, two plexi composing the ENS have been described: the myenteric (or Auerbach's) plexus and the submucosa (or Meissner's) plexus [48]. In addition, a third plexus (pelvic plexus) is found at the posterior end of the gut; it is visible in cross-section between the colon and Fabricius bursa (Figure 13B'', arrow). The myenteric plexus is localized between the longitudinal and circular muscle layer (Figures 13C'' and D'', MP) driving gut motility. The submucosa plexus (Figures 13C'' and D'', SP) on the submucosa layer provides secretomotor innervation to the mucosa, close to the lumen of the gut. These two plexi are connected together by neurons extensions (visible in Figure 13C'' as small dots) that innervate the circular muscle layer, allowing a proper innervation of all muscle layers.

At E13, PROX1 is not detected within the gut mesenchyme (Figure 13B''', arrow). However, we find it expressed next to it inside the pelvic plexus, a structure labeled by the TUJ1 antibody (Figure 13B’’’, arrow). Its pattern of expression and its colocalization with TUJ1 are unexpected, as it clearly does not label a lymphatic vascular structure, and no PROX1 expression has ever been reported in this region.

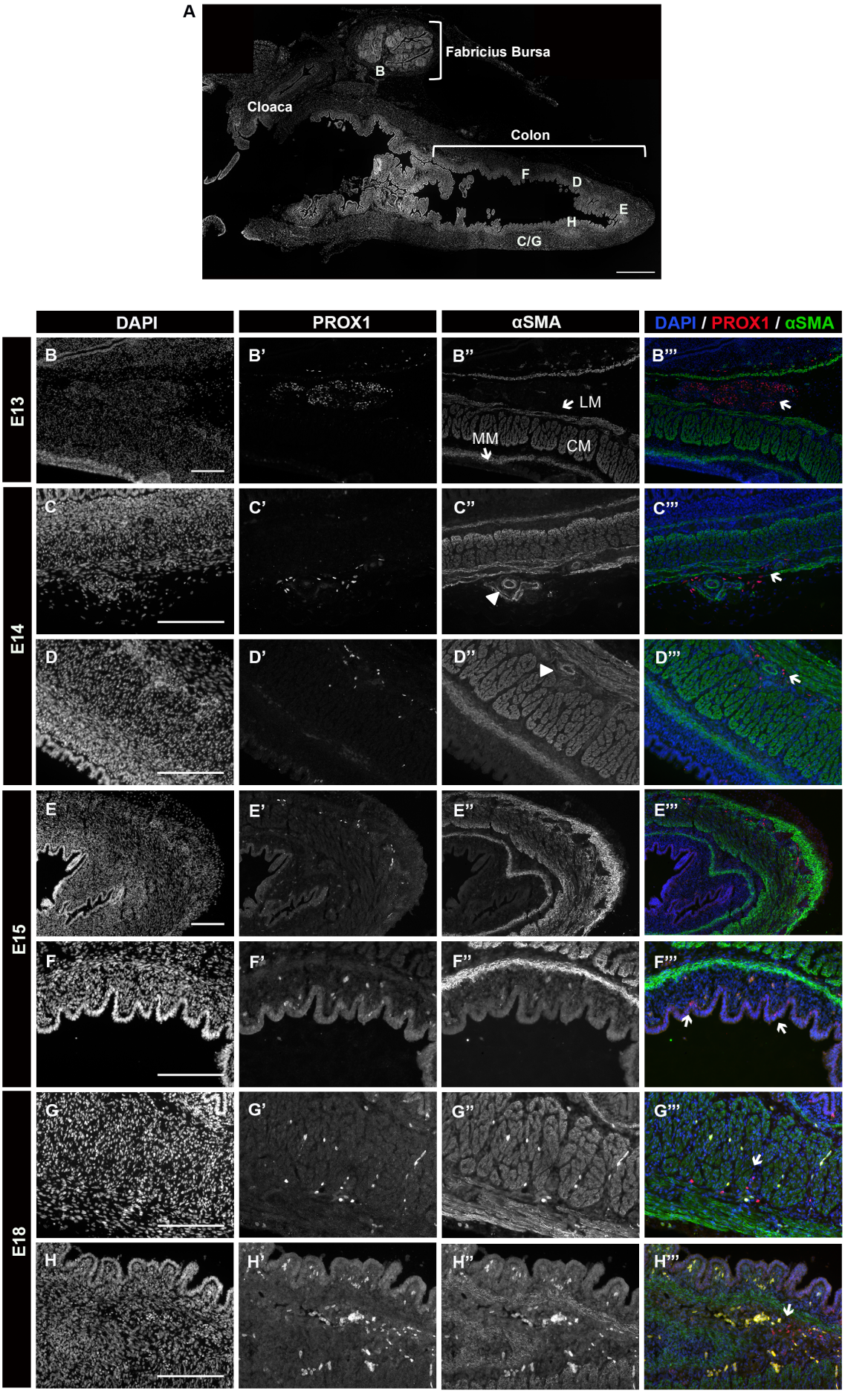
A
Fabricius Bursa
B
Cloaca
Colon
F
D
E
H
C/G
DAPI
PROX1
αSMA
DAPI / PROX1 / αSMA
E13
E14
E15
E18
B
B'
B''
B'''
LM
MM
CM
C
C'
C''
C'''
D
D'
D''
D'''
E
E'
E''
E'''
F
F'
F''
F'''
G
G'
G''
G'''
H
H'
H''
H'''

Figure 12 - Characterization of lymphatic system development in relation to the blood vasculature and smooth muscles.
Immunohistochemistry study performed on sagittal sections of E13 to E18 colon samples (A). LS was visualized with PROX1 antibody (B'-H') while blood vessels and smooth muscle layers with αSMA (B''-H''). Three different layers of muscle are present from the outer to the inner of colon: longitudinal muscle layer (B'',LM), circular muscle layer (B'',CM) and muscularis mucosa layer (B'',MM). The LS develops from the outer networks close to blood vessels (C'',D'', arrowheads). At E14, it appears to be invading the colon between the outer most muscle layer down to the muscularis mucosa muscle layer close to the epithelium (C''',D''',G''',H''', arrows). PROX1 expression in some epithelial cells is not related to LS (F''', arrows). Autofluorescence of red blood cells is observed in yellow/orange (F'''-H''').
Scale bar: 600µm (A); 150µm (B-H).

At E14, PROX1 is found expressed in lymphatic vessels present in the outer most layers of the gut and (as previously shown in Figures 12C''' and D'''), this lymphatic network extends within the colon into and between the two muscle layers, and along the myenteric plexus (Figures 13C''' and D'''). At E15, LEC are present close to the myenteric plexus while at E18 they have invaded the circular muscle (Figure 13F''', arrow) down to the submucosa, where they stand in close association with two other networks: the blood vasculature (Figure 13G''', arrowhead) and the ENS (Figure 13G''', SP). Interestingly, at E18 PROX1 is found in some epithelial cells not related to lymphatic vessels (Figure 13G''').

In this first part, we show that lymphangiogenesis in the digestive tract occurs relatively late during development (after E14). This was a real concern for the research project we wanted to initiate. Indeed, in the chick model the tools and techniques we use in the lab request manipulation on very young embryos (around E1.5). Although very useful for many stages, these manipulations result in a very high death rate on embryos after E9/E10, which is incompatible with the study as we originally designed it.

However, during our investigations we found a very interesting and unexpected place of expression for *PROX1* (see below). As this process occurs at a developmental stage that allows its study in the chicken model, we decided to move to this new project.

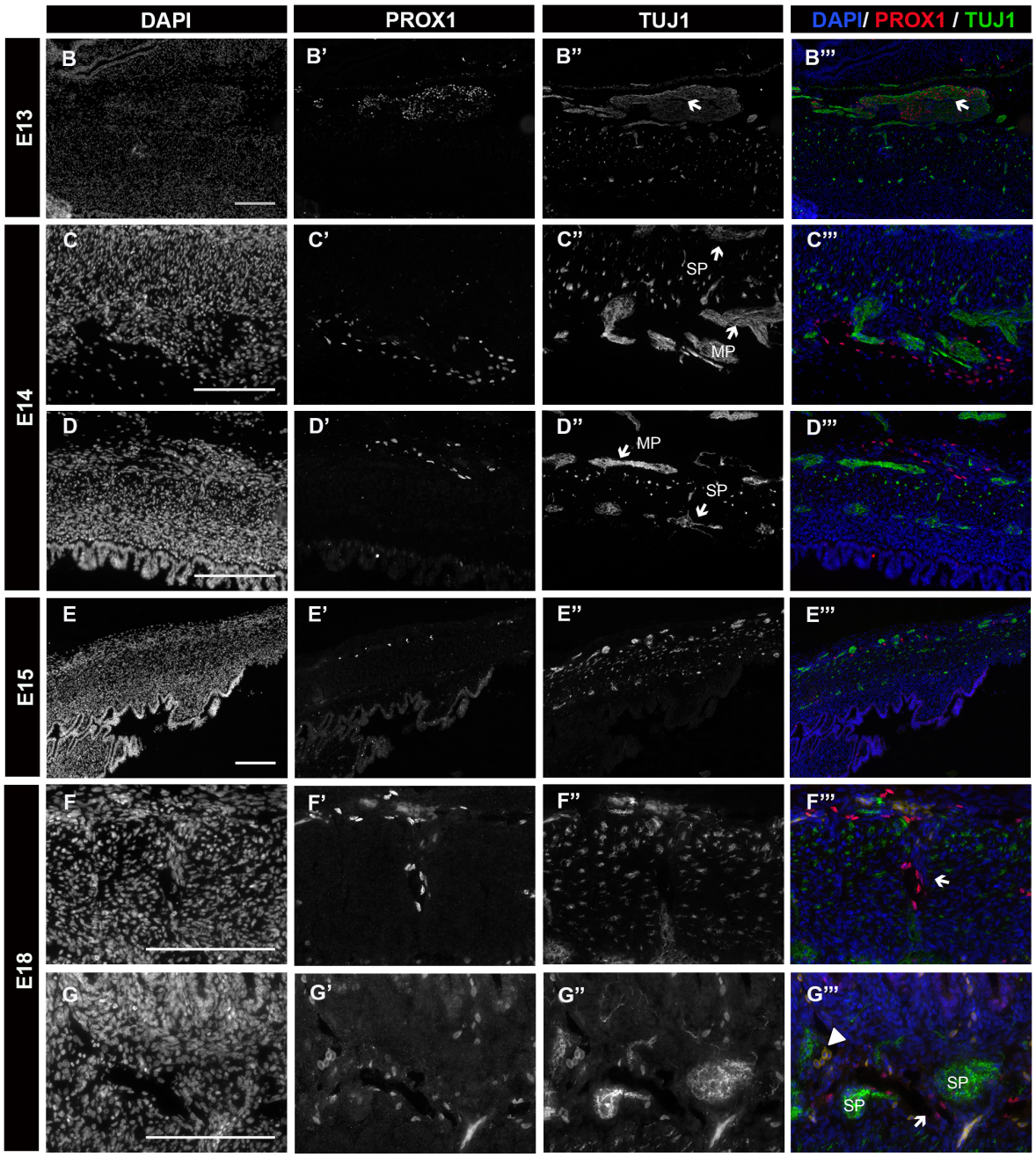

Figure 13 - Characterization of lymphatic system development in relation to the enteric nervous system.
Immunohistochemistry study was performed on sagittal sections of E13 to E18 colon samples (Figure 13A). LS was visualized with PROX1 antibody (B'-G') and ENS with TUJ1 (B''-G''). Two plexi are present from the outer to the inner of colon: myenteric plexus or Auerbach's (C'',MP) and submucosa plexus or Meissner's (C'',SP). LS is in close proximity to the ENS (F''',G''',arrows). PROX1 expression in pelvic plexus (B'',B''',arrows) and in some epithelial cells is not related to LS (G'''). Autofluorescence of red blood cell is seen in yellow, permitting to visualize the vascular system (G''',arrowhead). Scale bar: 150µm.

III.3. Sacral neural crest cells express *PROX1* in the nerve of Remak

While performing whole-mount ISH for *PROX1* at early stages of development, we found that it was expressed in a structure unrelated to the LS. This structure, which develops alongside the colon and one part of the small intestine, is called the nerve of Remak (NoR), and is a part of the ENS that originates from the sacral NCC [22]. So far, no marker allowing to distinguish between the two types of NCC (vagal and sacral) constituting the ENS has been found. In this regard, *PROX1* could be the first marker specific of sacral-derived ENS cells, and thus we decided to further characterize *PROX1* presence in the NoR. The NoR develops together with the gut from stage E4.5 [24] so we initiated our whole-mount ISH time course from E5 to E9.

To visualize the migration of both waves of NCC that constitute the ENS in the gut we used a probe detecting the expression of the *SOX10* gene (Figure 14). As we can see in Figure 14B, *SOX10* is already strongly expressed in the NoR at E5 and this expression is maintained in this structure at all the stages we studied (up to E9 - Figures 14D, F, H, J) and even later during development (data not shown). In contrast, *PROX1* expression is more dynamic during development. At E5 and E6 *PROX1* (Figures 14A and C) shows a strong expression in the NoR. However, from E7 (Figure 14E, G, I) this expression quickly decreases to be only faintly sustained in the pelvic plexus. It is also interesting to observe the wave of the *SOX10*-positive vagal NCC that colonize the gut in an antero-posterior manner. These cells are first detected in the cecum at E6 (VNCC, Figure 14D) progressively invading the whole cecum at E7 and the colon at E8 (VNCC, Figures 14F and H), and finally reaching the most posterior part of the gut by E9 (VNCC, Figure 14J).

In parallel, to confirm our ISH studies, we performed a quantitative RT-PCR analysis to quantify the expression level of both genes during development. These results correlate with the observation made by ISH, showing a peak in *PROX1* expression in the colon at E6, and progressively decreasing at E7, E8 and E9 (Figure 15A). On the other hand, *SOX10* expression in the colon increases at every developmental stage reflecting the progressive colonization by the vagal and sacral NCC (Figure 15B).

An interesting correlation is observed: *PROX1* downregulation takes place when sacral derived cells from the NoR start migrating into the colon, around E7-E8. To find whether this downregulation is also observed at the protein level, we moved to immunohistochemistry assays on colon cross-sections from E6 to E9.5 with PROX1 and TUJ1 (a neuron specific β-tubulin) antibodies (Figure 16). TUJ1, is used to label sacral and vagal NCC.

At E6-E7 (Figures 16B'',C'',D'') the only population of NCC visible is the one in the NoR (sacral NCC). At E7.5 nerve fibers derived from the NoR and expressing TUJ1 enter the colon external to the circular muscle layer, at the level of the presumptive myenteric plexus (MP, Figure 16E''). Vagal NCC are known to migrate in an antero-posterior wave and from the submucosal to the myenteric plexus. On the contrary, sacral NCC migrate from the posterior to the anterior part of the gut (up to the umbilical part) colonizing the myenteric plexus first [4,22,23].

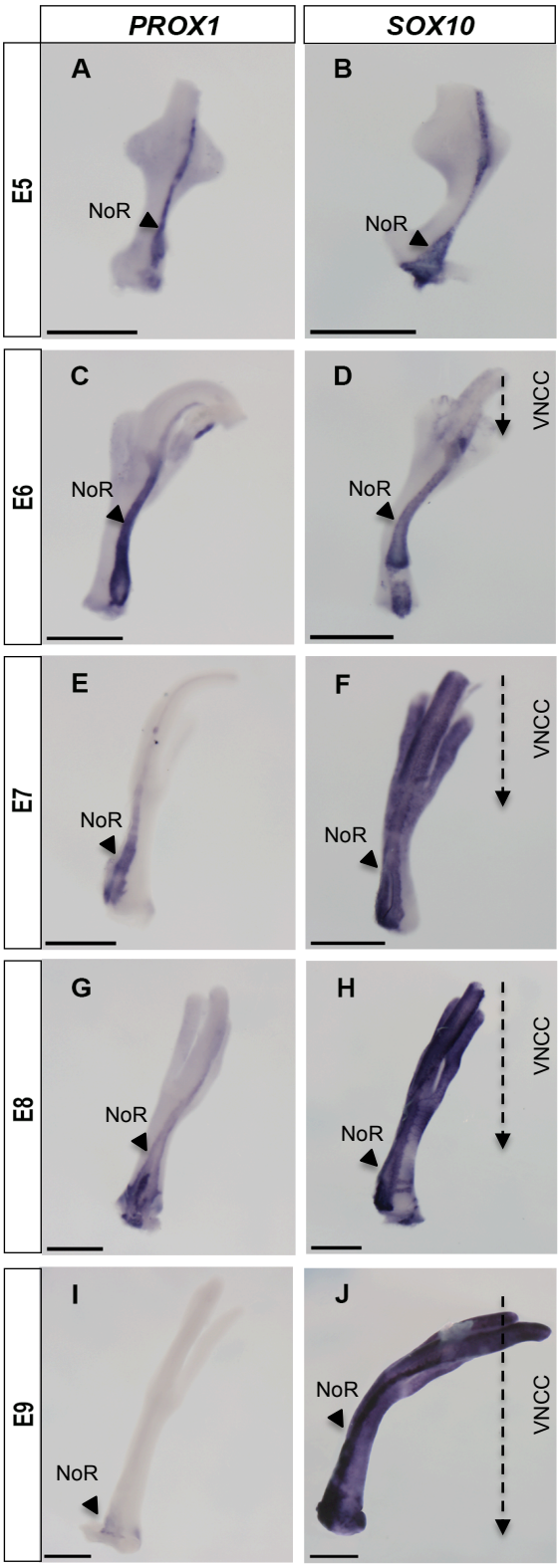

Figure 14 - *PROX1* is expressed in the nerve of Remak at early stages of embryonic development.

At E5, *PROX1* is expressed in the NoR (arrowheads NoR), which is seen by *SOX10* expression in an ENS structure (arrowheads NoR). The NoR is only constituted by sacral NCC but another type, vagal NCC, is also migrating towards the end of colon (dashed arrows, VNCC). After E6, *PROX1* starts being downregulated until E9 when it is no longer seen. At E9, vagal NCC have colonized the entire colon. Scale bar: 1mm

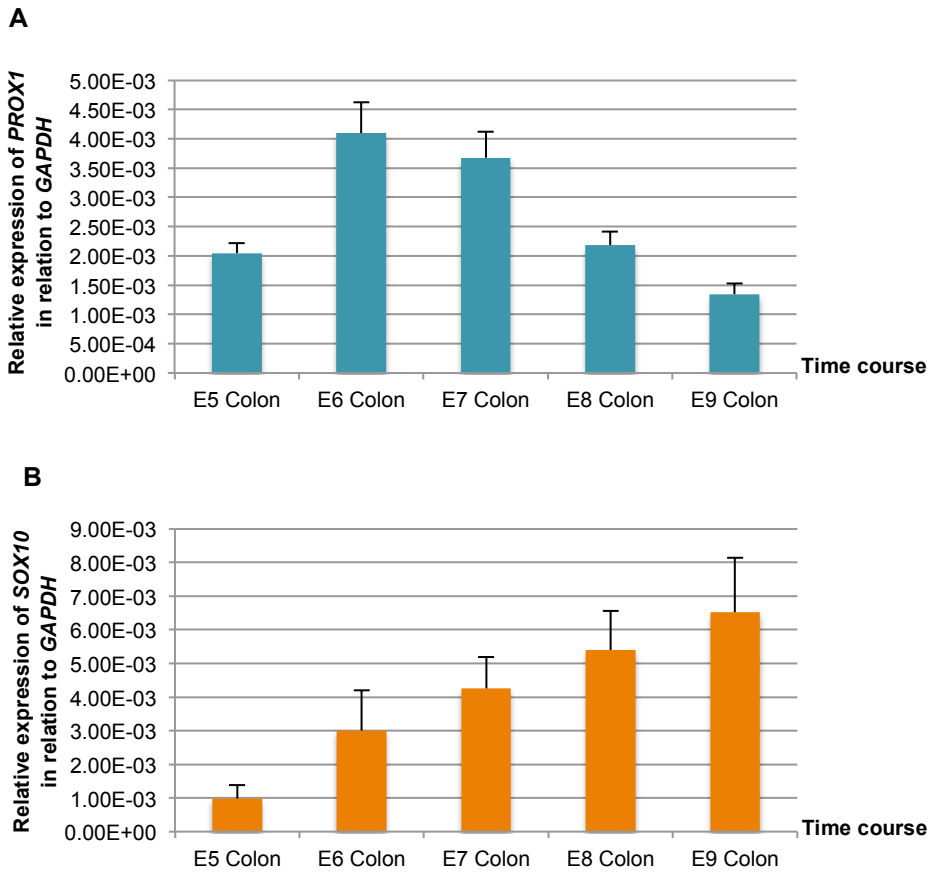

Figure 15 – The peak of *PROX1* expression occurs at E6 on the colon.
Quantitive analysis of *PROX1* expression reveals a higher expression of this gene at E6, being downregulated afterwards (A). *SOX10* expression increases along the time course due to sacral and vagal NCC colonization (B). In the graphics, mean values±s.e.m are shown relative to *GAPDH* control. Each measurement was done on three independent cDNA preparations.

From E8 these two NCC derived populations are present in the colon with two plexus visible (Figures 16F'',G'',H'',I'', MP and SP) and at E8.5 we observe fibers connecting the myenteric and submucosal plexus (Figure 16G'', arrowhead).

In agreement with the quantitative RT-PCR results (Figure 15), at E6 there is a peak of PROX1 protein in the NoR (Figure 16B'). This peak diminishes, as the organ develops. Around E7.5-E8, PROX1 protein decreases in a more noticeable way, correlating with sacral NCC entrance into the colon (Compare Figure 16E' with E'' and Figure 16F' with F''). PROX1 positive cells that are not positive for TUJ1 are LEC (Figures 16B',C',D',E',G',H',I', arrows).

It is interesting to note that PROX1 protein was never observed in nerve fibers projecting from the NoR. At E9 and E9.5 (Figures H' and I') only very few cells still have PROX1 protein, which is in correlation with absence of gene expression at this stage (Figure 14I); and suggesting that somehow PROX1 is impeding the entrance of sacral NCC into the colon.

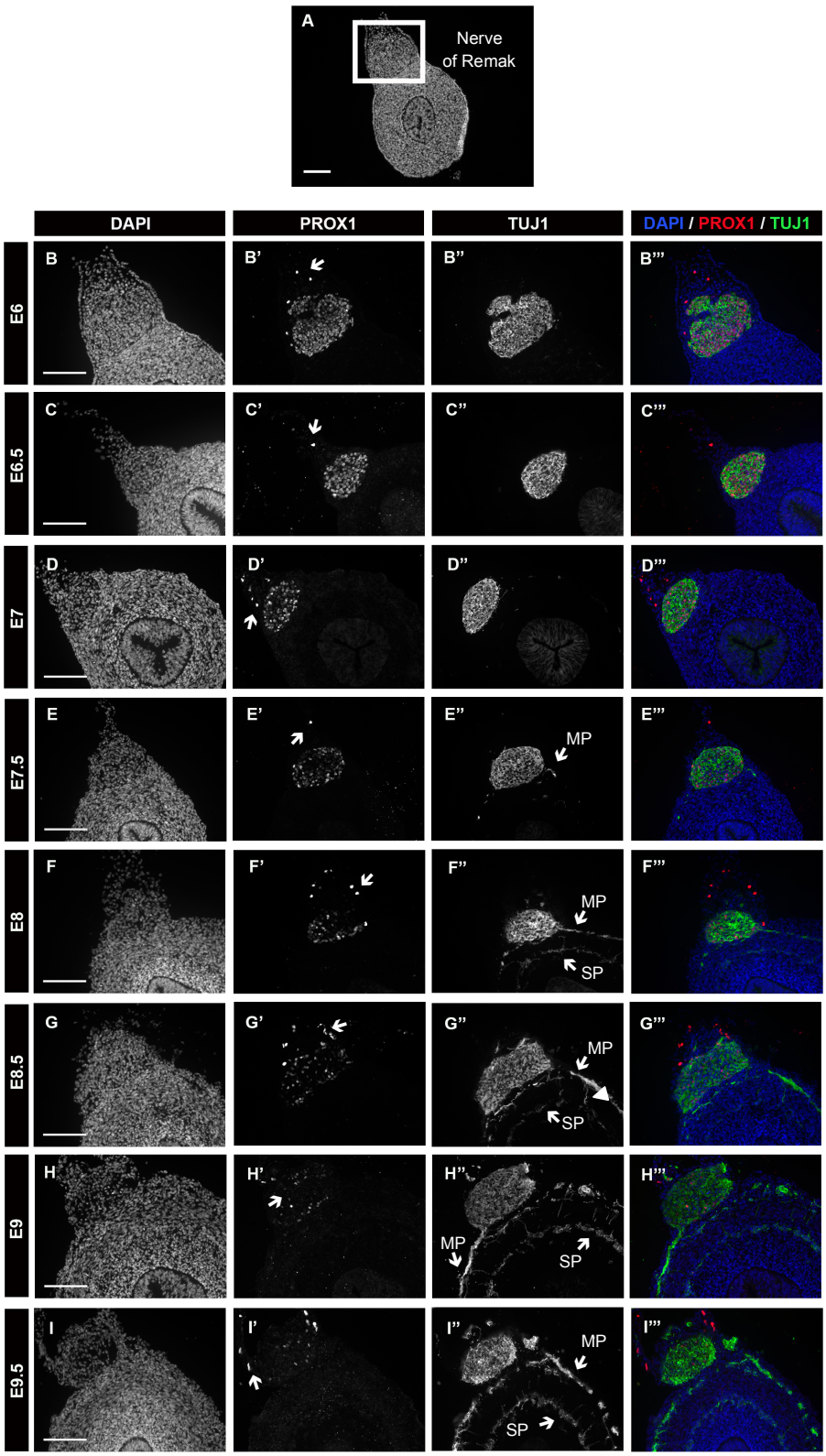

Figure 16 - PROX1 protein decrease is correlated with sacral neural crest cells entrance into the colon.

Immunhistochemistry technique was done on transversal sections of E6-E9.5 colons to visualize the NoR (A). PROX1 and TUJ1 antibodies were used to evaluate PROX1 dynamics and ENS migration along the time course. Two enteric plexus are present: myenteric (MP) and submucosa plexus (SP) and when PROX1 decreases in the nerve, sacral NCC migrate to the plexus (F',F''). Additional PROX1 staining, outside the nerve, represents the LEC (B',C',D',E',F',G',H',I', arrows). Scale bar: 150µm.

In order to determine if cells expressing *PROX1* in the NoR are directly derived from the sacral NCC, we undertook three different approaches. The first approach was based on an *in vitro* assay, using a drug treatment that chemically ablates the ENS and look for its effects on *PROX1* expression. After a dissection at E6.5, organs were treated with a benzalkonium chloride solution (BAC) and cultured for 48 hours in a differentiation medium. ISH on samples dissected at E6.5 show that colons were not entirely colonized by vagal NCC (Figure 17A, asterisk) with a migration front located just after the cecum, while sacral NCC were present in the NoR (Figure 17A, arrowhead). The NoR was also expressing *PROX1* at that stage, as shown in Figure 17B, arrowhead.

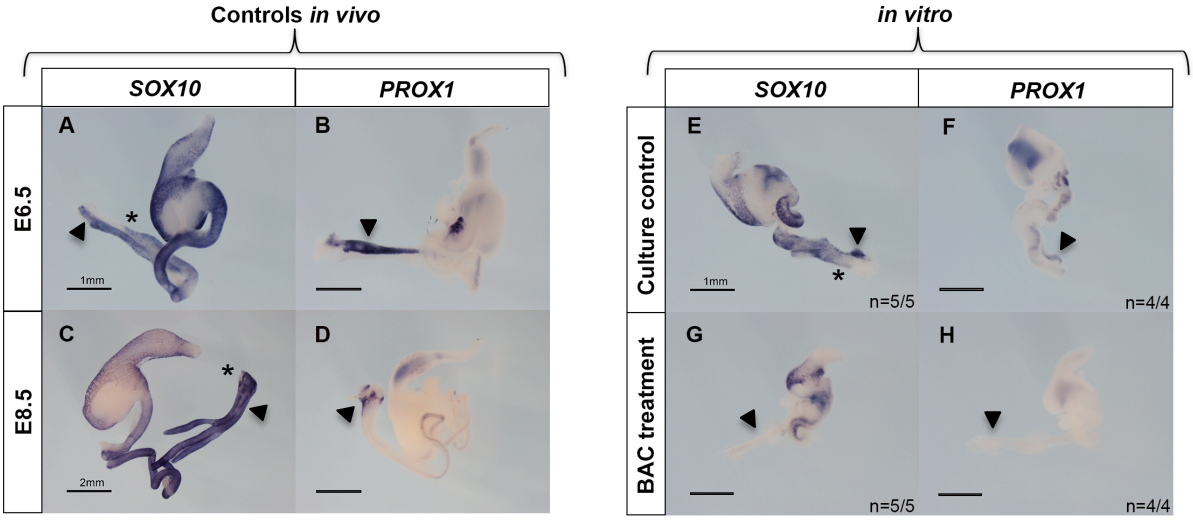

Figure 17 - Chemical death of sacral neural crest cells causes absence of *PROX1* expression in the nerve of Remak.
Organ culture with benzalkonium chloride solution was used to kill ENS of E6.5 guts (A,B) and at E8.5 effects were assessed with *SOX10* and *PROX1* probes (E-H). Culture conditions and E8.5 control (C,D) were not in the exact same stage of development but still a difference is observable between the two culture conditions. Sacral NCC (arrowheads) deletion leads to absence of *PROX1* into the NoR (G,H). Vagal NCC front of migration is seen with asterisks. Scale bar: 1mm (A,B,E-H), 2mm (C,D).

When dissected at E8.5 *SOX10* is expressed within the whole colon and NoR (Figure 17C), while *PROX1* expression is restricted to the pelvic plexus (Figure 17D).

Comparing E8.5 controls with culture controls (untreated guts cultured for 48 hours) a difference of staging is perceptible (compare Figures 17C and D with 17E and F). Indeed, in the E8.5 control, vagal NCC have colonized the entire gut, while in the culture control, their migration has only reached the middle of the colon. In the E8.5 control, *PROX1* is restricted to the pelvic plexus, whilst in the culture control it is still expressed within the NoR. This means that organ culture samples were delayed in development by about 12 to 24 hours, showing a developmental stage of E7.5-E8 (compare Figures 17E and F with 14E-H). Despite these staging issues between E8.5 controls and culture conditions, we were still able to observe that organs placed

in organ culture followed their development with ENS cells migrating more posterior and *PROX1* expression starting to decrease as expected. Interestingly, if we now compare culture controls with BAC treated guts (Figures 17E and G), we observe a clear decrease in *SOX10* expression, especially in the NoR and colon (n=5/5), indicating a loss of NCC in these areas. Regarding *PROX1,* its expression was completely lost under these conditions (n=4/4) (Figures 17F and H). From this experiment, we can conclude that in the organ culture experiment, when we induce neuronal cell death with the BAC treatment, the expression of *PROX1* is strongly inhibited.

To further confirm our results, we decided to use a second approach consisting of an *in vivo* genetic ablation of sacral NCC (Figure 18). In this experiment, we injected and electroporated an U2-*DTA* plasmid into the caudal neural tube, at the level of somite 25 and caudalward at the developmental stage HH16 (about E2.5). This construction allows the expression of the diphtheria toxin, in all cells expressing *SOX10*, and thus kills every NCC receiving the construct. As the microinjection was done at the sacral level of the neural tube, only sacral NCC and not vagal NCC were affected. After microinjection/electroporation embryos were placed back in the incubator until they reached E6.5; then colons were dissected and RNA extracted for quantitative RT-PCR analysis. As described in Figure 18A, *SOX10* expression decreases by 14.6% in the colon of electroporated embryos compared to *GFP* electroporated controls, thus validating the technique. In these animals, *PROX1* expression is reduced by 17.2% compared to controls (Figure 18B). In conclusion to this experiment we can say that decreasing the number of sacral NCC in the neural tube results in a reduction of *PROX1* expression in the NoR. Thus these results also suggest sacral NCC are the source of PROX1 expressing cells in the NoR.

Finally, a second *in vivo* approach was performed again with E2.5 embryos, in which the portion of neural tube located next to somite 25 and caudalward was ablated (Figure 19A). When successfully done, no sacral NCC are present within the gut [49], while in the case of a partial removal, the reduced number of sacral NCC would only allow the migration to the most posterior part of the gut and then the formation of a shorter NoR.

Embryos were dissected for analysis at E6.5, which corresponds to a stage where both RNA and protein for *SOX10* and *PROX1* are normally found in the NoR (Figures 19B and C; 16C-C'''). In our control, colon cross-sections show expression of both the neuronal marker TUJ1 and PROX1 in the NoR.

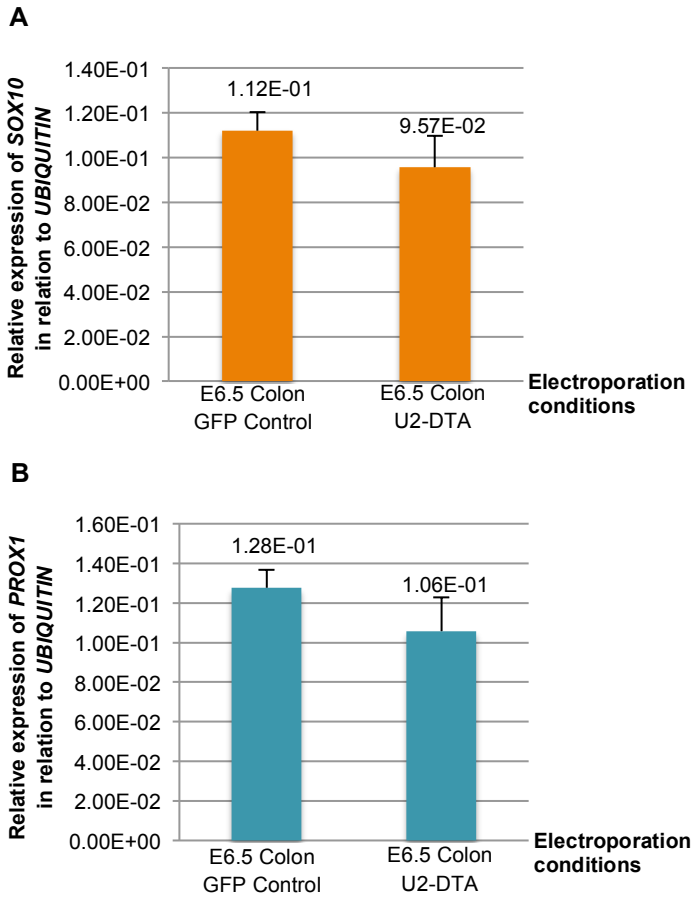

Figure 18 - U2-*DTA* plasmid electroporation into the sacral neural crest cells leads to a decrease of *PROX1* expression in the nerve of Remak.
SOX10 diminished 14.6% with an *in vivo* ablation of sacral NCC (A) and *PROX1* had a decrease of 17.2%. In the graphics, mean values±s.e.m are shown relative to *UBIQUITIN* control. Each measurement was done on three independent cDNA preparations.

This coexpression is found throughout the hindgut, in the anterior part of the cecum (Figure 19D""), the posterior part of the cecum (Figure 19E"") and in the colon (Figure 19F""). PROX1 positive cells that are not expressing a neuronal marker are LEC (Figures 19D" and F", arrows).

When evaluating ablated colons, a divergence depending on the level of the section along the antero-posterior axis is noticeable. In the most anterior part of the cecum (Figures 19G-G"") no NoR is seen with TUJ1 staining, and PROX1 is absent as well. As we move more posteriorly along the hindgut, the NoR with its TUJ1 and PROX1 expression are present (Figures 19H-H"" and I-I""). This shows that when partially ablated, sacral NCC migrate a shorter distance along the hindgut, and that this loss of sacral NCC in this region is associated with a loss of *PROX1* expression.

In conclusion to our *in vitro* and *in vivo* approaches, we can confirm our hypothesis that *PROX1* is expressed in the NoR, by the cells derived from the sacral NCC. These results make *PROX1* the first specific marker of the sacral derived cells of the ENS.

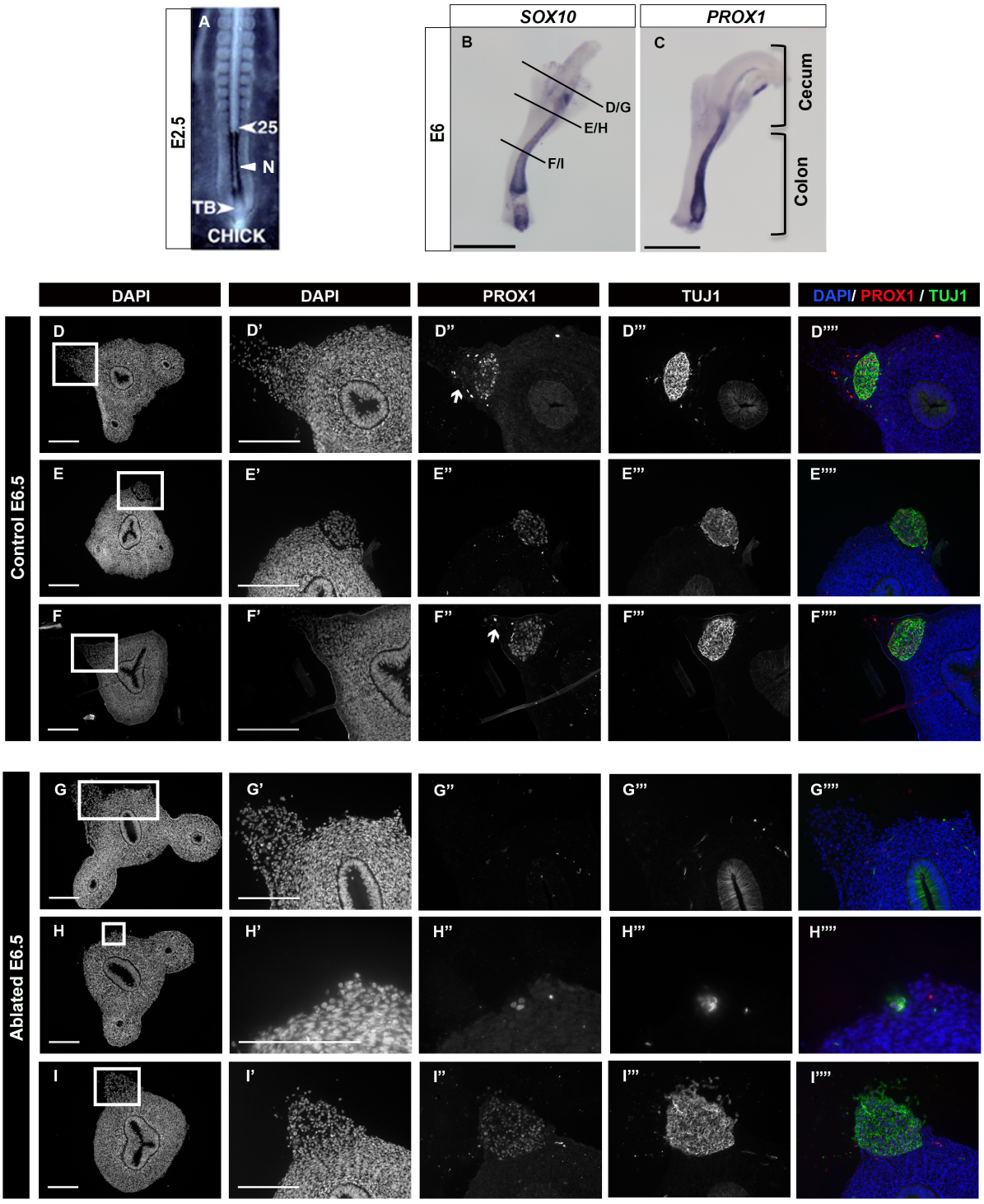

Figure 19 - Surgical ablation of the end part of the neural tube, causes absence of the nerve of Remak formation and a decrease of *PROX1* expression.

Surgical ablation was done as demonstrated in A on E2.5 embryos and effects assessment were interpreted at E6.5 embryonic stage with recourse to immunohistochemistry, since at E6, *PROX1* has been seen to be expressed in the nerve (B,C).

Different levels along the colon were analyzed and all showed PROX1 in the nerve in control samples (D"",F""). PROX1 marked by arrows is LEC (D",F"). In ablated samples and depending on section's localization along the antero-posterior axis, the nerve was (G"',H"') or was not ablated (I"'). Where the nerve was not present PROX1 was also absent (G",H"). This heterogeneous result in the same colon is due to non-complete ablation of the end part of the neural tube. Figure A was adapted from [24]. N= notochord; TB= tail bud.

Scale bar: 1mm (B,C), 150µm (D-I,D'-I').

III.4. Investigation of *PROX1* function in sacral neural crest cells/Nerve of Remak.

Given the correlation observed between PROX1 downregulation in the NoR and sacral NCC entrance into the colon, we hypothesized that PROX1 might be a regulator that determines when sacral NCC can migrate out of the nerve. To address this question we performed *in vivo* and *in vitro* assays including gain and lost-of function approaches both based on plasmid microinjection with *PROX1*- and ΔDBD-*PROX1*-pCIG4 constructs and electroporation (Figure 20).

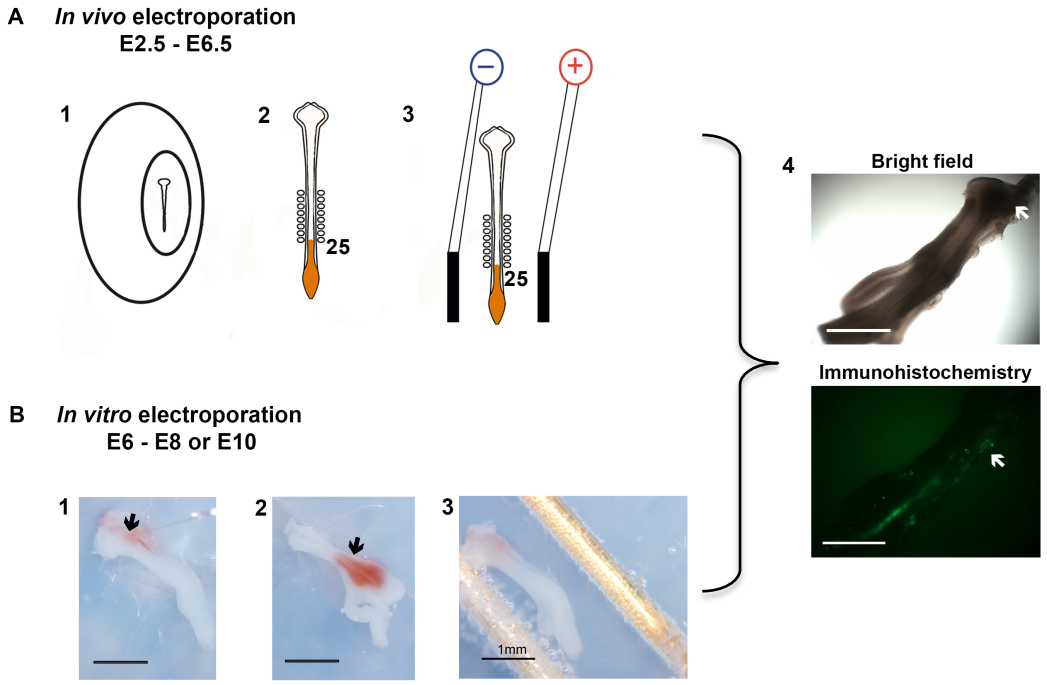

Figure 20 - Experimental design of plasmids electroporation into sacral neural crest cells to misregulate *PROX1* gene expression.
In vivo assays were done in E2.5 embryos with plasmids injection into the end part of neural tube, around somite 25 and caudalwards (A1-3). Schemes were adapted from [50]. Assessment of the effects should be done at E6.5 using colons that express GFP into the nerve (A4, arrows). *In vitro* experiments were done with E6 colons that were injected into the NoR (B1 and B2, arrows) and assessment of the effects should be done at E8 for ΔDBD-*PROX1* plasmid and E10 for *PROX1* plasmid. Electroporation was done bilaterally with 25V, 3 pulses of 5ms (A3,B3). Scale bar: 1mm.

The *in vivo* approach was done in embryos at stage HH16 (E2.5) injected into the neural tube from somite 25 and caudalwards, and incubated up to stage E6.5 (Figure 20A). When colons were dissected at E6.5 only the ones expressing *GFP* in the nerve were kept for immunohistochemistry assays (Figure 20, A4). To characterize the effect of misregulating *PROX1* expression in the NoR, two combinations of antibodies were used: anti-GFP with either PROX1 or TUJ1. Anti-GPF antibody is used to visualize electroporated cells. Due to experiment troubleshooting and time issues, it was not possible for me to analyze the samples with immunohistochemistry

technique as originally planned. However the expected results are detailed in Table 1.

The *in vitro* approach was performed only in the NoR of E6 colons that were left in culture for 2 days, when injected with ΔDBD-*PROX1*, and 4 days, when injected with *PROX1* (Figure 20B). The expected results for immunohistochemistry assays are detailed in Table 2 and Table 3.

Table 1 - Expected results of immunohistochemistry technique performed in electroporated E6.5 embryos. Experimental conditions (*PROX1* and ΔDBD-*PROX1*) should be compared to control *GFP* plasmid (pCIG4) in order to evaluate misregulation effects. Anti-GFP antibody should be used to visualize electroporated cells, which are misexpressing *PROX1* constructs. PROX1 and TUJ1 antibodies should be used to analyze the effects on the NoR in terms of *Prox1* expression and sacral NCC entrance towards the colon.

		Plasmid injected	Antibodies	Expected results
***In vitro* E2.5 - E6.5**	**CONTROL**	**pCIG4**	anti-GFP Mouse PROX1 Rabbit	Strong presence in the NoR
			anti-GFP Rabbit TUJ1 Mouse	Stains the NoR; Sacral NCC have not entered the colon
	EXPERIMENTAL CONDITIONS	***PROX1* + pCIG4**	anti-GFP Mouse PROX1 Rabbit	Same as control
			anti-GFP Rabbit TUJ1 Mouse	Same as control
		ΔDBD-*PROX1* + pCIG4	anti-GFP Mouse PROX1 Rabbit	Fewer PROX1 cells in the NoR and PROX1 detected in the colon
			anti-GFP Rabbit TUJ1 Mouse	Stains the NoR; Sacral NCC have already entered the colon

Regarding these last two approaches that we developed, we were not able to generate reproducible convincing data before I left the lab. However these experiments should provide us results that are sufficient to confirm (or invalidate) *PROX1* function in sacral NCC migration out of the NoR. If our hypothesis is validated, it will open new insights into the study of diseases related to ENS. *PROX1* being a transcription factor, this discovery could open the door for the identification of more new specific markers of sacral derived ENS. Unraveling new signaling pathways activated downstream of *PROX1* would provide new tools for the study of pathologies such as the Hirschsprung disease, but also help differentiate between the several types of colonic neuropathies which have been so far improperly characterized.

Table 2 - Expected results of immunohistochemistry technique performed in electroporated E8 colons with pCIG4 and ΔDBD-*PROX1*. This misregulation is estimated to cause an anticipation of sacral NCC entrance into the colon by annulment of *PROX1* inhibition effect on these cells. Anti-GFP antibody should be used to confirm electroporation localization and plasmid insertion. PROX1 and TUJ1 antibodies should be used to analyze the effects on the NoR in terms of *PROX1* expression and sacral NCC entrance towards the colon.

		Plasmid injected	Antibodies	Expected results
***In vitro* E6 - E8**	CONTROL	**pCIG4**	anti-GFP Mouse PROX1 Rabbit	Very few PROX1 staining in the NoR
			anti-GFP Rabbit TUJ1 Mouse	Stains the NoR; NCC are already present in two plexi
	EXPERIMENTAL CONDITIONS	**ΔDBD-*PROX1* + pCIG4**	anti-GFP Mouse PROX1 Rabbit	No staining in the NoR (if antibody does not recognize this altered form of PROX1); Eventually some PROX1 cells in the colon
			anti-GFP Rabbit TUJ1 Mouse	Stains the NoR; Myenteric plexus develops quicker

Table 3 - Expected results of immunohistochemistry technique performed in electroporated E10 colons with pCIG4 and *PROX1*. This misregulation is estimated to cause a delay of sacral NCC entrance into the colon by maintenance of *PROX1* inhibition effect on these cells. Anti-GFP antibody should be used to confirm electroporation localization and plasmid insertion. PROX1 and TUJ1 antibodies should be used to analyze the effects on the NoR in terms of *PROX1* expression and sacral NCC entrance towards the colon.

		Plasmid injected	Antibodies	Expected results
***In vitro* E6 - E10**	CONTROL	**pCIG4**	anti-GFP Mouse PROX1 Rabbit	No PROX1 in the NoR
			anti-GFP Rabbit TUJ1 Mouse	Stains the NoR; Plexi are well developed
	EXPERIMENTAL CONDITIONS	***PROX1* + pCIG4**	anti-GFP Mouse PROX1 Rabbit	PROX1 is still present in the NoR
			anti-GFP Rabbit TUJ1 Mouse	Stains the No; More sacral NCC in the NoR, and plexi inside colons (especially myenteric) are less developed

Chapter IV

DISCUSSION

The initial aim of our study was to investigate the mechanism of lymphatic development in the gut. Our results show that lymphatic vasculature within the intestine (Figure 9) develops much later than the cardiovascular system (Figure 8). In a way, this gap between both vasculature developments was predictable since, it has already been reported for the chick that there is an important delay between the initiation of angiogenesis from E1 and the first appearance of LECs on the jugular lymphatic sacs around E6.5 [51,52]. We found that lymphangiogenesis occurs quite late during the development of the gut (from E14), colonizing the gut from the mesentery and developing towards the innermost layers. During our investigations on lymphatic development we found that *PROX1*, a major lymphatic maker, was first expressed specifically in the NoR at early stages. This unsuspected expression pattern led us to investigate its expression pattern in more detail and we found that *PROX1* is a specific marker of the sacral NCC present in the NoR, which constitute together with the vagal NCC the precursor cells of the ENS.

IV.1. Gut lymphatic network development

Our results show an important delay in the formation of both vasculatures in the gut. Indeed no lymphatic structure is observed in the intestine before E14, while *CLAUDIN5* expression already highlighted the presence of a vascular network in the stomach and intestine at E5. We first observe lymphatic vessels in the gut between the longitudinal and circular muscle layer, close to the myenteric plexus at stage HH40 (E14). Then, in the E15 to E18 interval of time, lymphatic vessels slowly migrate towards the submucosa layer. A close proximity between the ENS and blood vessels has already been described, with conflicting results on whether the development of these two structures influence each other or not [53,54]. Here our results show at later stages, similar patterns with lymphatic vessels developing close to the ENS myenteric and submucosa plexi. Interestingly SEMAPHORIN members, a group of molecules implicated in axon guidance, and their receptors the NEUROPILINS, are required for both lymphangiogenesis and NCC migration. NEUROPILIN1 is expressed by vagal and sacral NCC that sense a SEMAPHORIN 3A gradient, which is known to inhibit axon growth of the NoR. When this gradient is retracted from all muscle layers into inner submucosa and mucosa layers, axons extend and sacral NCC migrate from these extensions into the colon [55]. In lymphatic vessels, *Neuropilin1* has been seen to be involved in valve formation [56]. Similarly, *Neuropilin2* is important for NCC migration [57] and as a co-receptor of VEGFR3 plays key-role during lymphangiogenesis [58]. Such similarities in pathway activation could in part explain such a close association during development.

What are the origins of gut lymphatic vessels: intrinsic or extrinsic? Recently, Winters[59] performed an interesting study about the origin and formation of the gut mesothelium, a simple squamous epithelium lined over the internal organs, which provides a non-adhesive surface for organ movement and is implicated in fluid movement and immune surveillance. They show that each mesothelium is derived from its own organ. When they performed chick-quail grafts of splanchnic mesoderm marked with GFP, labeled cells appeared on mesothelium, muscular layer and submucosa at E10. Staining of the mesothelium with αSMA and endothelial markers revealed that some GFP splanchnic mesoderm derived cells were positive for vascular αSMA and others were neither positive for αSMA nor endothelial markers. They could not characterize these last cells but if we remember that lymphatic vessels do not have αSMA surrounding them (only the big vessels are surrounded by αSMA) and that some lymphangioblasts were proved to be derived from mesenchyme and not endothelial cells, these cells could be gut lymphangioblasts candidates. While Wilting [51] reported a dual origin for jugular lymphatic system that would give rise to the lymphatic vasculature, Schneider [60] saw in one specimen that mesenchymal lymphangioblasts in the limb bud contributed to the jugular lymph sac without fusing first with jugular vein. These mesenchymal lymphangioblasts originate from PROX1-expressing cells in dermomyotomes [51] (Figure 21).

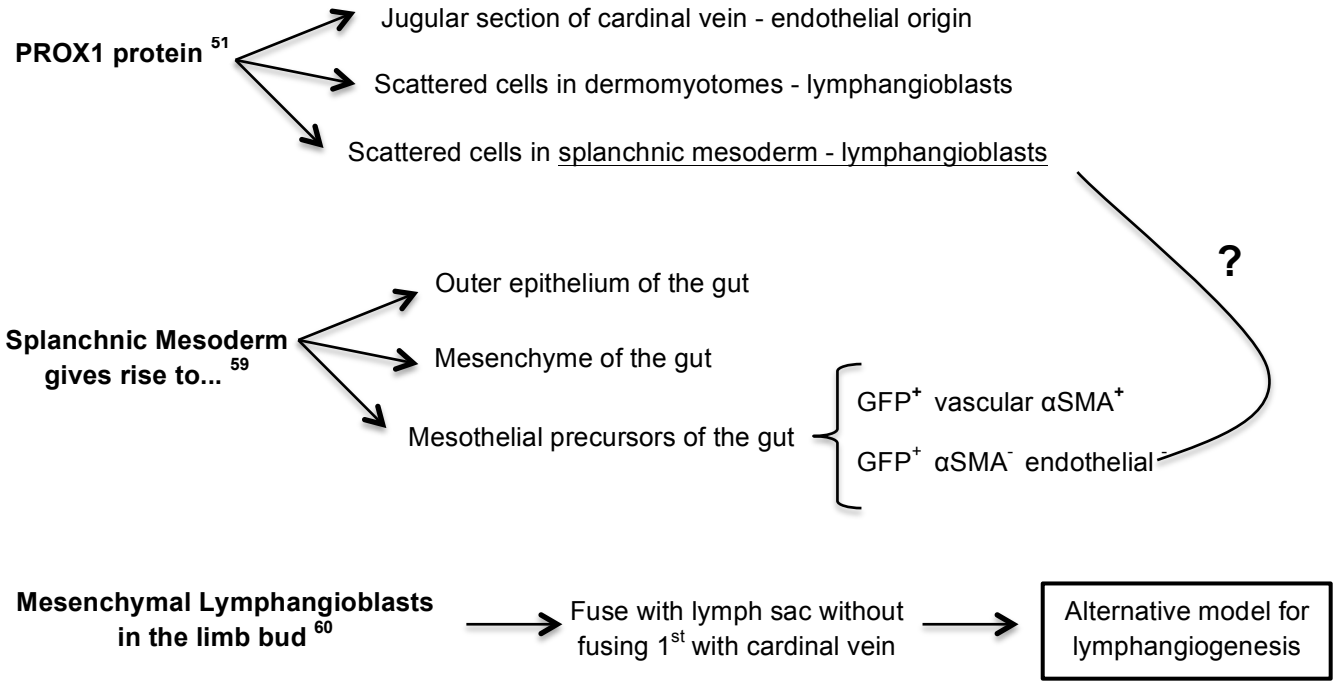

Figure 21 - Scheme of three studies hypothesizing an alternative model for lymphangiogenesis from lymphangioblasts.

If we hypothesize that PROX1 cells in the splanchnic mesoderm give rise to lymphangioblasts we could expect that the lymphatic network of the gut arises from these cells. They would fuse with the retroperitoneal (mesenteric) lymph sac, then extend and form the lymphatic vasculature within the gut and communicate with the rest of the body. In addition, we observe at E13 the expression of PROX1 in a few colonic smooth muscle cells of the circular and longitudinal muscles (data not shown). This expression is not consistent throughout the muscles but only exists in the layers next to the myenteric plexus. At E14 we already have some lymphatic vessels within these two muscles. These cells in combination with mesenteric lymph sac could give rise to the intestine's lymphatic vasculature.

IV.2. *PROX1* expression and function in the establishment of the sacral enteric nervous system.

Our results identified a novel marker of NCC, which allows distinction between vagal and sacral populations. The expression of *PROX1* is first observed in the NoR at E5, and is downregulated only when sacral NCC migrate into the colon/small intestine around E7-E8. This correlation is also visible with PROX1 protein, whose decrease is more noticeable around E7.5-E8. All of our different *in vivo* and *in vitro* approaches led us to the conclusion that *PROX1* expression in the NoR marks sacral NCC. Interestingly, no expression of *PROX1* was detected in *SOX10*-positive vagal NCC migrating antero-posteriorly at these stages. Such a specific marker has long been looked for. Delalande [24] showed for the first time a difference in expression between vagal and sacral NCC. Vagal NCC were seen expressing 4-fold higher *RET* mRNA levels than sacral NCC. From all candidate genes expressed by NCC this was the only noticeable difference. This unsuspected expression pattern opens the way for new studies, and the identification of PROX1 downstream targets will aid the discovery of more sacral NCC-specific markers, providing new tools for the characterization of colonic ENS associated pathologies.

Assuming that our expectations on Tables 1-3 are proved to be true, we would be showing that *PROX1* has a role in blocking sacral NCC inside the NoR. Given the fact that PROX1 protein has a homeodomain, this confers the property to both activate and repress transcription of other genes depending on the context.

Kaltezioti [44] showed both in chick and mouse that PROX1 in the neural tube represses NOTCH1. NOTCH1 signaling inhibits neurogenesis, thus PROX1 has a role in suppressing NOTCH1 activity, which leads to neural progenitor cell differentiation. NOTCH1 and SOX10 together maintain the ENS progenitor pool and later on promote gliogenesis. The difference between these two fates may result in additional regulatory mechanism acting in different developmental stages [61]. Our results show that from E5 to E9 *SOX10* is expressed in both NoR and migrating sacral and vagal NCC, while *PROX1* is only expressed between E5 and E8 before sacral NCC migration into the colon/small intestine. *PROX1* can be a candidate for this additional mechanism that regulates dual function of SOX10 and NOTCH1. One hypothesis is that before *PROX1* expression, SOX10 and NOTCH1 proteins are in the NoR maintaining the sacral NCC pool of progenitors. As soon as PROX1 protein

is present in the NoR, *NOTCH1* starts being downregulated which leads to initial neural differentiation. *PROX1* downregulation increases NOTCH1 protein levels again that together with SOX10 can now induce gliogenesis (Figure 22). However, even though NOTCH1 can also help in migration of NCC, when PROX1 is still in the NoR, there are already some sacral NCC migration waves into the colon. Another pathway also involved in ENS development is HEDGEHOG signaling, which also has a role in NCC migration and could inhibit the NOTCH pathway [61,62].

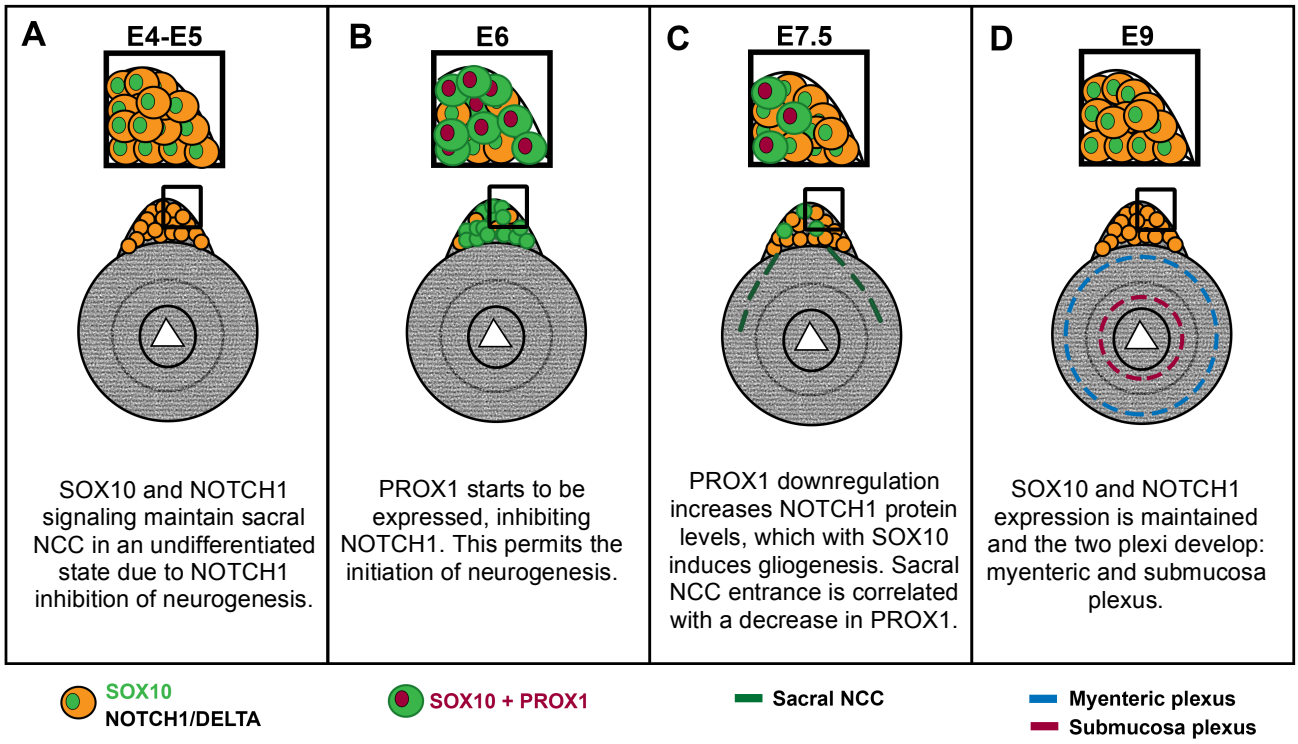

Figure 22 - Model for PROX1 function in sacral enteric nervous system establishment in the colon.
SOX10 and NOTCH1 maintain sacral NCC in an undifferentiated state due to the role of NOTCH1 signaling in inhibiting neurogenesis (A). Our results show that PROX1 levels become stronger around E6 and we propose that this transcriptor factor has a role in suppressing NOTCH1 activity, causing NOTCH1 downregulation. This would permit the initiation of neurogenesis (B). Our results also show that PROX1 levels decrease and cease around E7.5-E8, which would permit the upregulation of NOTCH1. PROX1 downregulation also correlates with sacral NCC entrance (C). At E9, PROX1 is absent in the colon and NOTCH1 and SOX10 activity correlates with gliogenesis. Myenteric and submucosa plexi are already established (D).

IV.3. Conclusions

In summary, our data show that *PROX1* plays a dual role during gut development. At early stages, it appears in the NoR and our hypothesis is that it could have a role in regulating either the initial migration of sacral NCC into the gut or their neural differentiation. At later stages, *PROX1* is not expressed in ENS structure anymore, but it is turned on in the lymphatic vasculature, where it is known to play key-roles in the regulation of its formation.

IV.4. Future prospects

In order to continue our study on *PROX1* function during ENS development, we will first need to conclude our misregulation experiments of *PROX1* in the NoR and validate the assumptions made in Tables 1-3. PROX1 being a transcription factor, the future step will be the identification of PROX1 transcriptional target genes. Given the specific expression of PROX1 in sacral NCC, this identification could provide us the opportunity to identify PROX1-target genes that could participate in conveying the specificity of sacral neural crest derived cell into the colon and small intestine. In addition, we will focus on PROX1-target genes, which maintain their expression in the colon in order to identify invaluable tools to discriminate sacral from vagal NCC in pediatric and adult human colon in order to investigate the contribution of sacral derived NCC in colonic ENS pathologies.

REFERENCES

1. Smith, D. M. *et al*. Evolutionary relationships between the amphibian, avian, and mammalian stomachs. *Evolution & Development* **2,** 348–359 (2000).
2. Hamburger, V. & Hamilton, HL. A series of normal stages in the development of the chick embryo.1951. *Dev. Dyn.* **195**, 231-271 (1992)
3. Bellairs, R. & Osmond, M. *Atlas of chick development* (2nd edition). Elsevier Academic Press. USA. (2005).
4. Le Douarin, N. M. & Teillet, M. A. The migration of neural crest cells to the wall of the digestive tract in avian embryo. *J Embryol Exp Morphol* **30,** 31–48 (1973).
5. Roberts, D. J., Smith, D. M., Goff, D. J. & Tabin, C. J. Epithelial-mesenchymal signaling during the regionalization of the chick gut. *Development* **125,** 2791–2801 (1998).
6. De Santa Barbara, P. & Roberts, D. J. Tail gut endoderm and gut/genitourinary/tail development: a new tissue-specific role for Hoxa13. *Development* **129,** 551–561 (2002).
7. Faure, S. *et al*. Expression pattern of the homeotic gene Bapx1 during early chick gastrointestinal tract development. *Gene Expr. Patterns* **13,** 287–292 (2013).
8. Young, H. M. & Newgreen, D. F. *Embryos, Genes and Birth Defects* (2nd edition). John Wiley & Sons. England. (2006).
9 Junqueira, L. & Carneiro, J. *Histologia Básica* (10ª edição). Guanabara Koogan. Rio de Janeiro. (2004)
10. Margaris, K. N. & Black, R. A. Modelling the lymphatic system: challenges and opportunities. *J R Soc Interface* **9,** 601–612 (2012).
11. Swartz, M. A., Hubbell, J. A. & Reddy, S. T. Lymphatic drainage function and its immunological implications: from dendritic cell homing to vaccine design. *Seminars in Immunology* **20,** 147–156 (2008).
12. Charman, W. N. & Stella, V. J. *Lymphatic Transport of Drugs*. CRC Press. USA. (1992).
13. Tammela, T. & Alitalo, K. Lymphangiogenesis: Molecular Mechanisms and Future Promise. *Cell* **140,** 460–476 (2010).
14. François, M. *et al.* Sox18 induces development of the lymphatic vasculature in mice. *Nature* **456,** 643–647 (2008).
15. Wigle, J. T. & Oliver, G. Prox1 function is required for the development of the murine lymphatic system. *Cell* **98,** 769–778 (1999).
16. Johnson, N. C. *et al.* Lymphatic endothelial cell identity is reversible and its maintenance requires Prox1 activity. *Genes & Development* **22,** 3282–3291 (2008).
17. François, M. *et al.* Segmental territories along the cardinal veins generate lymph sacs via a ballooning mechanism during embryonic lymphangiogenesis in mice. *Developmental Biology* **364,** 89–98 (2012).

18. Pan, Y., Wang, W.-D. & Yago, T. Transcriptional regulation of podoplanin expression by Prox1 in lymphatic endothelial cells. *Microvasc. Res.* **94,** 96–102 (2014).

19. Simons, M. & Eichmann, A. Physiology. Lymphatics are in my veins. *Science* **341,** 622–624 (2013).

20. Burns, A. J. & Pachnis, V. Development of the enteric nervous system: bringing together cells, signals and genes. *Neurogastroenterol Motil* **21,** 100–102 (2009).

21. Le Douarin, N. & Kalcheim, C. *The Neural Crest* (2nd edition). Cambridge University Press. UK. (1999).

22. Burns, A. J. & Douarin, N. M. The sacral neural crest contributes neurons and glia to the post-umbilical gut: spatiotemporal analysis of the development of the enteric nervous system. *Development* **125,** 4335–4347 (1998).

23. Conner, P. J. *et al*. Appearance of neurons and glia with respect to the wavefront during colonization of the avian gut by neural crest cells. *Dev. Dyn.* **226,** 91–98 (2003).

24. Delalande, J.-M. *et al.* The receptor tyrosine kinase RET regulates hindgut colonization by sacral neural crest cells. *Developmental Biology* **313,** 279–292 (2007).

25. Heanue, T. A. & Pachnis, V. Enteric nervous system development and Hirschsprung's disease: advances in genetic and stem cell studies. *Nat. Rev. Neurosci.* **8,** 466–479 (2007).

26. Amiel, J. & Lyonnet, S. Hirschsprung disease, associated syndromes, and genetics: a review. *J. Med. Genet.* **38,** 729–739 (2001).

27. Manié, S., Santoro, M., Fusco, A. & Billaud, M. The RET receptor: function in development and dysfunction in congenital malformation. *Trends Genet.* **17,** 580–589 (2001).

28. de Graaff, E. *et al.* Differential activities of the RET tyrosine kinase receptor isoforms during mammalian embryogenesis. *Genes & Development* **15,** 2433–2444 (2001).

29. Taraviras, S. *et al.* Signalling by the RET receptor tyrosine kinase and its role in the development of the mammalian enteric nervous system. *Development* **126,** 2785–2797 (1999).

30. Chalazonitis, A. *et al*. Age-Dependent Differences in the Effects of GDNF and NT-3 on the Development of Neurons and Glia from Neural Crest-Derived Precursors Immunoselected from the Fetal Rat Gut: Expression of GFRα-1 in Vitro and in Vivo. *Developmental Biology* **204,** 385–406 (1998).

31. Hearn, C. J., Murphy, M. & Newgreen, D. GDNF and ET-3 differentially modulate the numbers of avian enteric neural crest cells and enteric neurons in vitro. *Developmental Biology* **197,** 93–105 (1998).

32. Heuckeroth, R. O. *et al*. Neurturin and GDNF Promote Proliferation and Survival of Enteric Neuron and Glial Progenitors in Vitro. *Developmental Biology* **200,** 116–129 (1998).

33. Natarajan, D. *et al*. Requirement of signalling by receptor tyrosine kinase RET for the directed migration of enteric nervous system progenitor cells during mammalian embryogenesis. *Development* **129,** 5151–5160 (2002).

34. Young, H. M. *et al.* GDNF is a chemoattractant for enteric neural cells. *Developmental Biology* **229,** 503–516 (2001).

35. Burns, A. J. & Thapar, N. Advances in ontogeny of the enteric nervous system. *Neurogastroenterol Motil* **18,** 876–887 (2006).

36. Bordeaux, M. C. *et al.* The RET proto-oncogene induces apoptosis: a novel mechanism for Hirschsprung disease. *The EMBO Journal* **19,** 4056–4063 (2000).

37. Barlow, A., de Graaff, E. & Pachnis, V. Enteric nervous system progenitors are coordinately controlled by the G protein-coupled receptor EDNRB and the receptor tyrosine kinase RET. *Neuron* **40,** 905–916 (2003).

38. Leibl, M. A. *et al.* Expression of endothelin 3 by mesenchymal cells of embryonic mouse caecum. *Gut* **44,** 246–252 (1999).

39. Sidebotham, E. L. *et al.* Localization and endothelin-3 dependence of stem cells of the enteric nervous system in the embryonic colon. *Journal of pediatric surgery* **37,** 145–150 (2002).

40. Kruger, G. M. *et al.* Temporally distinct requirements for endothelin receptor B in the generation and migration of gut neural crest stem cells. *Neuron* **40,** 917–929 (2003).

41. Cantrell, V. A. *et al.* Interactions between Sox10 and EdnrB modulate penetrance and severity of aganglionosis in the Sox10Dom mouse model of Hirschsprung disease. *Hum. Mol. Genet.* **13,** 2289–2301 (2004).

42. Zhu, L. *et al.* Spatiotemporal regulation of endothelin receptor-B by SOX10 in neural crest-derived enteric neuron precursors. *Nat. Genet.* **36,** 732–737 (2004).

43. Streit, A. & Stern. C. Combined whole-mount in situ hybridization and immunohistochemistry in avian embryos. *Methods* **23,** 339-344 (2001).

44. Kaltezioti, V. *et al.* Prox1 Regulates the Notch1-Mediated Inhibition of Neurogenesis. *PLoS Biol* **8,** e1000565 (2010).

45. Rios, A. C. *et al.* Neural crest regulates myogenesis through the transient activation of NOTCH. *Nature* **473,** 532–535 (2011).

46. Westmoreland, J. J. *et al.* Pancreas-specific deletion of Prox1 affects development and disrupts homeostasis of the exocrine pancreas. *Gastroenterology* **142,** 999–1009.e6 (2012).

47. Shyer, A. E. *et al.* Villification: how the gut gets its villi. *Science* **342,** 212–218 (2013).

48. Doyle, A. M., Roberts, D. J. & Goldstein, A. M. Enteric nervous system patterning in the avian hindgut. *Developmental Dynamics* **229,** 708–712 (2004).

49. Burns, A. J., Delalande, J.-M. M. & Le Douarin, N. M. In ovo transplantation of enteric nervous system precursors from vagal to sacral neural crest results in extensive hindgut colonisation. *Development* **129,** 2785–2796 (2002).

50. Itasaki, N., Bel-Vialar, S. & Krumlauf, R. 'Shocking' developments in chick embryology: electroporation and in ovo gene expression. *Nat. Cell Biol.* **1,** E203–7 (1999).

51. Wilting, J. *et al.* Dual origin of avian lymphatics. *Developmental Biology* **292,** 165–173 (2006).

52. Pardanaud, L. *et al*. Vasculogenesis in the early quail blastodisc as studied with a monoclonal antibody recognizing endothelial cells. *Development* **100,** 339–349 (1987).

53. Delalande, J.-M. *et al.* Vascularisation is not necessary for gut colonization by enteric neural crest cells. *Developmental Biology* **385,** 220–229 (2014).

54. Nagy, N. *et al.* Endothelial cells promote migration and proliferation of enteric neural crest cells via beta1 integrin signaling. *Developmental Biology* **330,** 263–272 (2009).

55. Shepherd, I. T. & Raper, J. A. Collapsin-1/semaphorin D is a repellent for chick ganglion of Remak axons. *Developmental Biology* **212,** 42–53 (1999).

56. Jurisic, G. *et al.* An unexpected role of semaphorin3a-neuropilin-1 signaling in lymphatic vessel maturation and valve formation. *Circ. Res.* **111,** 426–436 (2012).

57. Gammill, L. S., Gonzalez, C., Gu, C. & Bronner-Fraser, M. Guidance of trunk neural crest migration requires neuropilin 2/semaphorin 3F signaling. *Development* **133,** 99–106 (2006).

58. Yuan, L. *et al.* Abnormal lymphatic vessel development in neuropilin 2 mutant mice. *Development* **129,** 4797–4806 (2002).

59. Winters, N. I., Thomason, R. T. & Bader, D. M. Identification of a novel developmental mechanism in the generation of mesothelia. *Development* **139,** 2926–2934 (2012).

60. Schneider, M. *et al*. Lymphangioblasts in the avian wing bud. *Dev. Dyn.* **216,** 311–319 (1999).

61. Liu, J. A.-J. & Ngan, E. S.-W. Hedgehog and Notch Signaling in Enteric Nervous System Development. *Neurosignals* **22,** 1–13 (2013).

62. Kim, T.-H. *et al*. Endodermal Hedgehog signals modulate Notch pathway activity in the developing digestive tract mesenchyme. *Development* **138,** 3225–3233 (2011).

Annex A

PROTOCOLS

A1 - cDNA production / RT-PCR (Thermo Scientific kit)

1. Put the eppendorf containing the total RNA at 70ºC for 5 minutes and then on ice.
2. Prepare the reverse transcription mix and only add the RNA in the end.

4 µL 5X cDNA synthesis buffer
2 µL dNTP Mix
1 µL RNA Primer
1 µL Reverse Transcriptase Enhancer
1 µL Verso Enzyme Mix
1 µg of Template RNA
RNase free water (Sigma-Aldrich)
Final volume = 20 µL

3. Incubate for 30/35 minutes at 42ºC.
4. Inactivate the enzyme at 95ºC for 2 minutes and stop the reaction on ice.

A2 - Primer design

NCBI database was used to obtain the mRNA sequences (http://www.ncbi.nlm.nih.gov/nuccore). Forward and reverse primers specific to each gene were designed (www.ncbi.nlm.nhi.gov/tools/primer-blast) and sequences (Annex B, Table B1) were aligned (http://blast.ncbi.nlm.nih.gov/Blast.cgi) to confirm the specificity of the final RNA probe.

A3 - PCR reaction and product ligation into plasmid

For each of our genes of interest, cDNA was amplified by PCR reaction from total cDNA, using gene specific forward and reverse primers. PCR conditions are detailed in Annex B, Table B2. Correct PCR products size were confirmed on a **2% agarose gel** (see Annex C for all the recipes) before being inserted into the linearized plasmid: pGEM®-T Easy Vector Systems (Promega; Annex D) for *LYVE1*, *PODOPLANIN* and *PROX1* or pBluescript® SK2 (Stratagene; Annex D) for *SOX10*. After bacterial transformation and miniprep amplification, plasmids were sent to sequencing to confirm sequences and determine cDNA orientation into the plasmid.

A4 - Bacteria transformation

10-15 ng of plasmid (in a maximum volume of 5 µL) was added to 50 µL of DH5α competent cells and incubated on ice for 30 minutes. A 42°C heat-shock was done for 40 seconds, and the reaction was immediately stopped on ice for 5 minutes. A first bacterial amplification step was done in 1 mL of LB medium without antibiotics for 1 hour at 37ºC. Then 200 µL of these bacteria were pipetted and plated on a **LB agar plate with ampicillin**, and left overnight at 37ºC. After an overnight culture, individual colonies were selected and PCR screened to confirm cDNA insertion (Annex B, Table B3).

A5 - Plasmid amplification and extraction

A single colony was picked from the selective plate and added to 3 mL of LB medium with ampicillin (miniprep). It was then placed overnight on a rocker (220 rpm) at 37ºC to allow bacterial growth. 1 mL of the miniprep was diluted in 50 mL of LB medium with ampicillin (maxiprep) and grown overnight again at 37°C. The next day plasmid extraction was carried out using the NucleoBond (Macherey-Nagel) kit, and was ressuspended in 100 µL of buffer TE. Plasmids were stored at -20°C.

A6 - Chick embryo powder [43]

1. Collect E7 chicken embryos (eye-less).
2. Homogenize them in a minimal volume of ice-cold calcium and magnesium-free phosphate-buffered saline, pH 7.4 with a homogenizer or a syringe.
3. Add 4 volumes of ice-cold acetone mix and incubate on ice for 30min.
4. Centrifuge at 10.000g for 10min and discard the supernatant.
5. Wash the pellet once with ice-cold acetone and spin again.
6. Spread the pellet out on Whatman filter paper and grind to a fine powder using a pestle.
7. Let it air dry and store at 4ºC.

Annex B

TABLES

Table B1 - List of forward and reverse primers used in *in situ* hybridization probe production.

RNA	Primer Forward	Primer Reverse
LYVE1	AAGGCAATCTCAGACGTGGTC	AGTGGGGATACCTCCAAAGACA
PODOPLANIN	AGTTATCATCCGTGCAAACCTCT	ACTGCTTTCAGGGCGAGTACC
PROX1	TGTAAAGTTCAACAGATGCATTACC	ATGTTAAGGGTCTCGGGCAA
SOX10	GCATCGGACAACTCTTCG	CCAGTCATAGCCGCTA

Table B2 - PCR program for amplification of the genes of interest.

Temperature	Time	
95ºC	60 seconds	
95ºC	60 seconds	35 cycles
60ºC	60 seconds	
72ºC	60 seconds / kb	
72ºC	10 minutes	

Table B3 - PCR program to screen cDNA insertion into the bacteria.

Temperature	Time	
95ºC	5 minutes	
95ºC	60 seconds	35 cycles
60ºC	60 seconds	
72ºC	60 seconds / kb	
72ºC	10 minutes	

Table B4 - List of RNA polymerases and restriction enzymes according to each gene of interest.

Gene	RNA polymerase (Roche)	Restriction enzyme (New England Biolabs)
CLAUDIN5	T3	Xba1
LYVE1	SP6	Apa1
PODOPLANIN	T7	SalI
PROX1	T7	Pst1
SOX10	T3	EcoRV

Table B5 - Time of fixation used according to embryo stage.

Embryo stage	Time used with 4% PFA
<E9	30 minutes
[E9;E12]	45 minutes
>E12	1 hour

Table B6 - Time used for proteinase K treatment according to embryo stage.

Embryo stage	Time used of Proteinase K
[E6;E7]	15 minutes
[E8;E9]	20 minutes
[E10;E16]	30 minutes

Table B7 - List of forward and reverse primers used in quantitative RT-PCR technique.

Gene	Primer Forward	Primer Reverse
GAPDH	CGTCCTCTCTGGCAAAG	TCACGCTCCTGGAAGATAG
UBIQUITIN	GGGATGCAGATCTTCGTGAAA	CTTGCCAGCAAAGATCAACCTT
PROX1	AATCTCGCCCTACTCGGGAA	GGTAATGCATCTGTTGAACTTTACA
SOX10	GCATCGGACAACTCTTCG	CCAGTCATAGCCGCTA

Annex C

RECIPES

- **2% agarose gel**
  0.5X TBE
  Agarose (2 gr per 100mL of TBE)
  4 µL/100 mL Ethidium Bromide

- **LB agar with ampicillin (1L)**
  10 g Tryptone
  5 g Yeast extract
  10 g NaCl
  ddH_20
  100 µg/mL Ampicillin

- **Hybridization solution**
  50% Formamide
  5X SSC, pH 4.5
  1% SDS
  50 µg/mL Yeast tRNA
  50 µg/mL Heparin
  DEPC treated water

- **Solution 1**
  50% Formamide
  5X SSC, pH 4.5
  1% SDS
  DEPC treated water

- **Solution 2**
  50% Formamide
  2X SSC, pH 4.5
  DEPC treated water

- **1X TBST - Levamisole**
  0.14 M NaCl
  2.7 mM KCl
  25 mM TrisHCl, pH 7.5
  O.1% Tween
  2 mM levamisole
  DEPC treated water

- **DEPC-treated water**
  2 L ddH_2O
  200 µL Diethyl pyrocarbonate

- **LT 100X**
  10% Tween
  0.2 M Levamisole=tetramisole hydrochloryde
  DEPC treated water

- **0.12 M Phosphate buffer**
  0.12 mM $CaCl_2$
  0.077 mM Na_2HPO_4
  0.023 mM NaH_2PO_4

- **Solution T1**
  4% Sucrose
  0.12 M Phosphate buffer
  DEPC treated water

- **Solution T2**
  15% Sucrose
  0.12 M Phosphate buffer

- **Solution T3**
  15% Sucrose
  7.5% Porcine gelatin
  0.12 M Phosphate buffer

- **Laemmli 4X buffer (10mL)**
  2 mL 1M Tris-HCl; pH 6.8
  0.8 g SDS
  4 mL 10% Glycerol
  0.4 mL 14.7M β-Mercaptoethanol
  1 mL 0.5 M EDTA
  8 mg Bromophenol Blue

- **Stacking gel (for 1 gel)**
  0.480 mL Acrylamide 40%
  0.260 mL Bis-acrylamide 2%
  0.630 mL Tris, pH=6.8
  25 µL SDS 20%
  25 µL APS10%
  5 µL Temed
  3.575 mL ddH_2O

- **12% SDS-PAGE running gel (for 1 gel)**
  3 mL Acrylamide 40%
  1.6 mL Bis-acrylamide 2%
  3.75 mL Tris, pH=8.8
  50 µL SDS 20%
  50 µL APS10%
  5 µL Temed
  1.55 mL ddH_2O

- **10X Running buffer**
  380 mM Glycine
  500 mM Tris Base
  1% SDS 20%

- **10X Transfer buffer**
  500 mM Glycine
  380 mM Tris base

- **1X Transfer buffer (1L)**
  100 mL 10X transfer buffer
  200 mL ethanol
  700 mL ddH_20

Annex D

PLASMID MAPS

D1 - pGEM®-T Easy Vector Systems (Promega)

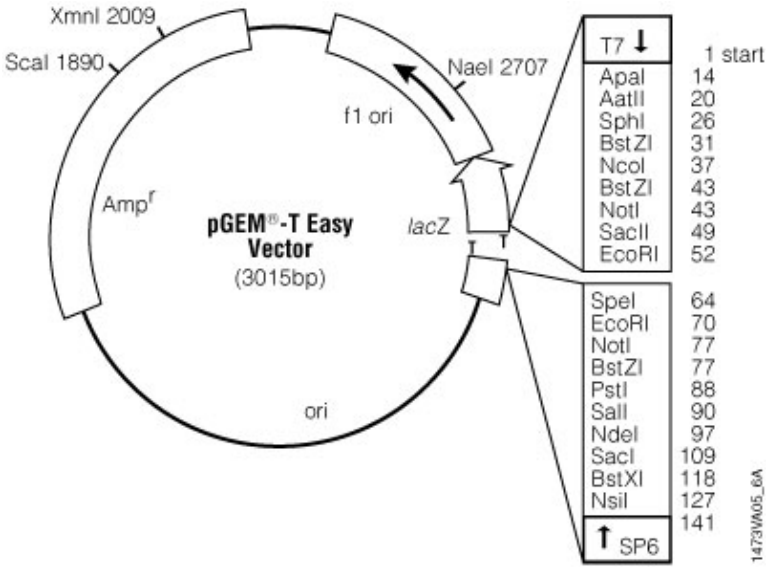

D2 - pBluescript® SK2 (Stratagene)

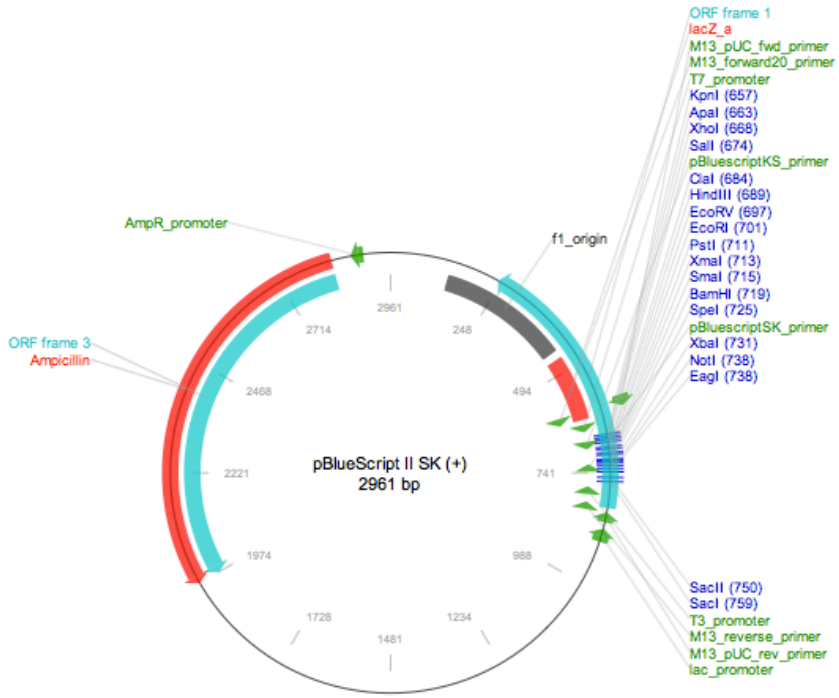

D3 - pCIG4 plasmid (Grapin lab, Denmark)